SIAM J. APPL. MATH.
Vol. 70, No. 1, pp. 77–111

THE REACTION-DIFFUSION MASTER EQUATION AS AN ASYMPTOTIC APPROXIMATION OF DIFFUSION TO A SMALL TARGET*

SAMUEL A. ISAACSON†

Abstract. The reaction-diffusion master equation (RDME) has recently been used as a model for biological systems in which both noise in the chemical reaction process and diffusion in space of the reacting molecules is important. In the RDME, space is partitioned by a mesh into a collection of voxels. There is an unanswered question as to how solutions depend on the mesh spacing. To have confidence in using the RDME to draw conclusions about biological systems, we would like to know that it approximates a reasonable physical model for appropriately chosen mesh spacings. This issue is investigated by studying the dependence on mesh spacing of solutions to the RDME in $\mathbb{R}^3$ for the bimolecular reaction $A + B \to \varnothing$, with one molecule of species A and one molecule of species B present initially. We prove that in the continuum limit the molecules never react and simply diffuse relative to each other. Nevertheless, we show that the RDME with nonzero lattice spacing yields an asymptotic approximation to a specific spatially continuous diffusion limited reaction (SCDLR) model. We demonstrate that for realistic biological parameters it is possible to find mesh spacings such that the relative error between asymptotic approximations to the solutions of the RDME and the SCDLR models is less than one percent.

Key words. reaction-diffusion, stochastic chemical kinetics, diffusion (limited) vacation, master equation

AMS subject classifications. 82C20, 82C22, 82C31, 41A60, 65M06

DOI. 10.1137/070705039

1. Introduction.

Noise in the chemical reaction process can play an important role in the dynamics of biochemical systems. In the field of molecular cell biology, this has been convincingly demonstrated both experimentally and through mathematical modeling. The pioneering work of Arkin and McAdams [7] has been followed by numerous studies showing that not only must biological cells compensate for noisy biochemical gene/signaling networks [12, 31, 40, 37], but they may also take advantage of the inherent stochasticity in the chemical reaction process [8, 44, 33].

Until recently, *stochastic* mathematical models of biochemical reactions within biological cells were primarily nonspatial, treating the cell as a well-mixed volume, or perhaps as several well-mixed compartments (i.e., cytosol, nucleus, endoplasmic reticulum, etc.). Biological cells contain incredibly complex spatial environments, comprised of numerous organelles, irregular membrane structures, fibrous actin networks, long directed microtubule bundles, and many other geometrically complex structures. While few authors have modeled the effects of these structures on the dynamics of chemical reactions within biological cells, several have recently begun to investigate what effect the spatially distributed nature of the cell has on biochemical signaling networks [42, 2, 38, 17, 47]. Deterministic reaction-diffusion PDE models are well established for modeling biochemical systems in which reactant species are present in

*Received by the editors October 10, 2007; accepted for publication (in revised form) January 12, 2009; published electronically May 1, 2009. Numerical simulations that stimulated this work made use of supercomputer time on the NCSA Teragrid system awarded under grant DMS040022.
http://www.siam.org/journals/siap/70-1/70503.html
†Department of Mathematics and Statistics, Boston University, 111 Cummington St., Boston, MA 02215 (isaacson@math.bu.edu). The author was supported by an NSF RTG postdoctoral fellowship when this work was carried out.

sufficiently high concentrations; however, there is not yet a standard model for systems in which noise in the chemical reaction process is thought to be important. Three different, but related, mathematical models [6, 28, 15, 48] have recently been used for representing stochastic reaction-diffusion systems in biological cells [2, 38, 17, 47].

In both the methods of [6] and [48], molecules are modeled as points undergoing spatially continuous Brownian motion, with bimolecular chemical reactions occurring instantly when the molecules pass within specified reaction-radii. We subsequently refer to this model, proposed by Smoluchowski [43], as a spatially continuous diffusion limited reaction (SCDLR). The approaches of [6] and [48] differ in their numerical simulation algorithms, but both involve approximations that remain spatially continuous while introducing time discretizations. In contrast to both these methods, the reaction-diffusion master equation (RDME) model used in [15] and [28] discretizes space, approximating the diffusion of molecules as a continuous-time random walk on a lattice, with bimolecular reactions occurring with a fixed probability per unit time for molecules within the *same* voxel (i.e., at the same lattice site). Exact realizations of the RDME can be created using the Gillespie method [21]. The method of [28] shows how to modify the diffusive jump rates of the standard RDME approach to account for complex spatial geometries.

While several authors have recently used the RDME to study biological systems (see, for example, [17] and [11]), there is still an unanswered question as to whether this spatially discrete model approximates any underlying physical model for appropriately chosen mesh sizes. (Note that [11] uses an approximate simulation algorithm instead of the exact Gillespie method approach mentioned above.) In particular, the main justification for the use and accuracy of the RDME appears to be the physical separation-of-timescales argument given in section 1.1.2. This argument suggests that the RDME is only *physically* valid for mesh sizes that are neither too large nor too small, and gives no hint as to an underlying spatially continuous model that is approximated by the RDME.

Our purpose herein is to investigate the dependence of the RDME on mesh spacing. We begin by answering the question of what happens in the continuum limit where the mesh spacing approaches zero. To this end, we prove in section 2.1 that for two molecules that can undergo the bimolecular reaction $\mathrm{A} + \mathrm{B} \to \varnothing$, as the mesh spacing approaches zero the molecules never react and simply diffuse relative to each other. This rigorous result appears to contradict the naive formal continuum limit,

$$D\Delta - k\delta(\boldsymbol{x}), \tag{1.1}$$

that one obtains for the generator of the dynamics (2.7). The apparent contradiction arises from the subtlety of giving a rigorous mathematical definition to the operator (1.1). In the context of quantum mechanical scattering in $\mathbb{R}^3$, an equivalent operator, with the reaction term called a pseudopotential, has been introduced formally by Fermi [19] and elaborated on by Huang and Yang [24]. A rigorous mathematical definition of (1.1) was first given by Berezin and Faddeev [10] and more recently by Albeverio, Brzeźniak, and Dąbrowski [3]. An important point in the work of [3] is that a one-parameter family of self-adjoint operators, $\Delta + \alpha\delta(\boldsymbol{x})$, may be defined in $\mathbb{R}^3$ corresponding to an extension of the standard Laplacian from $\mathbb{R}^3 \setminus \{(0,0,0)\}$ to $\mathbb{R}^3$. The results of section 2.1 imply that the standard scaling of the bimolecular reaction rate used in the RDME leads the solution of the RDME to converge to the $\alpha = 0$ operator, i.e., the Laplacian on $\mathbb{R}^3$. To obtain an operator (1.1) corresponding to the formal continuum limit that differs from the Laplacian, one would need to

appropriately renormalize the bimolecular reaction rate and/or extend the reaction operator to couple in neighboring voxels.

We next investigate what the RDME approximates for mesh spacings that are neither too large nor too small. The operator (1.1) arises in quantum mechanics to give local potentials whose scattering approximates that of a hard sphere of a fixed radius. Here, the dynamics (2.7) generated by a physically appropriate, mathematically rigorous definition of (1.1) provides an asymptotic approximation in the reaction-radius to the solution of the SCDLR model. This motivates section 2.2, where we show that when the mesh spacing is larger than an appropriately chosen reaction-radius, defined by the relative diffusion constant and bimolecular reaction rate of the species, the RDME is an asymptotic approximation in the reaction-radius to the SCDLR model [43, 29]. We derive, for the special case of two molecules that can undergo the bimolecular reaction $\mathrm{A} + \mathrm{B} \to \varnothing$, asymptotic expansions in the reaction-radius of the solutions to both the RDME and the SCDLR model in subsections 2.2.1 and 2.2.2, respectively. In subsection 2.2.3 we prove that the zeroth- and first order terms in the expansion of the RDME converge to the corresponding terms of the SCDLR model, while the second order term diverges. Moreover, we examine the numerical error between the expansion of the RDME, truncated after the second order term, and the asymptotic expansion of the SCDLR model, also truncated after the second order term. It is shown that for biologically relevant values of the reaction-radius the relative error between the two truncated expansions can be reduced below one percent with appropriately chosen mesh widths. This *suggests* that for biologically relevant parameter regimes and well-chosen mesh spacings, the RDME might provide a useful approximation to the SCDLR model.

The model problem studied in section 2 is chosen for ease of mathematical analysis. We believe that our results should be extendable to the general RDME formulation presented in section 1.1 for chemical systems with arbitrary zeroth-, first-, and second order chemical reactions. Note that for a general chemical system the RDME is a, possibly infinite, coupled system of ODEs. Formally, as we show in [26], the continuum limit of the coupled system is equivalent to a, possibly infinite, coupled system of PDEs with distributional coefficients. Similarly, a number of authors [39, 46] have exploited the equivalence of the RDME to a discrete version of the second quantization Fock-space formulation of Doi [14] to study formal representations of the continuum limit of the RDME.

1.1. Background on the RDME. We begin by formulating the RDME in subsection 1.1.1. A recent review of stochastic reaction-diffusion models and numerical methods, including the RDME, is provided in [16]. In subsection 1.1.2 we present a standard physical argument for determining mesh sizes where the RDME should be a "reasonable" physical model. Subsection 1.1.3 briefly reviews the relationship between deterministic reaction-diffusion PDE models and the RDME.

1.1.1. Mathematical formulation. We consider the stochastic reaction and diffusion of chemical species within a domain, Ω. Ω may denote a closed volume or all of $\mathbb{R}^3$. In the RDME model, Ω is divided by a mesh into a collection of voxels labeled by vectors $\boldsymbol{i}$ in some index set I (i.e., $\boldsymbol{i} \in I$). For example, if $\Omega = \mathbb{R}^3$, then $I = \mathbb{Z}^3$. It is assumed that the size of each voxel can be chosen such that within each voxel, independently, the well-mixed formulation of stochastic chemical kinetics [34] is physically valid. Determining for which mesh sizes this supposition is reasonable is one of the main goals of this work, and is further discussed in sections 1.1.2 and 2. Given this assumption, diffusive transitions of particles *between* voxels are then modeled as

first order chemical reactions. Note that this is equivalent to modeling diffusion as a continuous-time random walk on a lattice.

The state of the chemical system of interest is defined to be the number of each chemical species within each voxel. Let $M_{\boldsymbol{i}}^l(t)$ denote the random variable for the number of particles of chemical species l in the $\boldsymbol{i}$th voxel, $l = 1, \ldots, L$. We define $\boldsymbol{M_i}(t) = \left(M_{\boldsymbol{i}}^1, \ldots, M_{\boldsymbol{i}}^L\right)$ to be the state vector of the chemical species in the $\boldsymbol{i}$th voxel, and $\boldsymbol{M}(t) = \{\boldsymbol{M_i}\}_{\boldsymbol{i}\in I}$ to be the total state of the system (i.e., the number of all species at all locations). The probability that $\boldsymbol{M}(t)$ has the value $\boldsymbol{m}$ at time t, given the initial state, $\boldsymbol{M}(0) = \boldsymbol{m}_0$, is denoted by

$$P(\boldsymbol{m}, t) \equiv \text{Prob}\{\boldsymbol{M}(t) = \boldsymbol{m} | \boldsymbol{M}(0) = \boldsymbol{m}_0\}.$$

We now define a notation to represent changes of state due to diffusive transitions. Let $1_{\boldsymbol{i}}^l$ be the state where the number of all chemical species at all locations is zero, except for the lth chemical species at the $\boldsymbol{i}$th location, which is one. (I.e., $\boldsymbol{M}(t) + 1_{\boldsymbol{i}}^l$ would add one to chemical species l in the voxel labeled by $\boldsymbol{i}$.) $k_{\boldsymbol{ij}}^l$ shall denote the diffusive jump rate for each individual molecule of the lth chemical species into voxel $\boldsymbol{i}$ from voxel $\boldsymbol{j}$, for $\boldsymbol{i} \neq \boldsymbol{j}$. Since diffusion is treated as a first order reaction and molecules are assumed to diffuse independently, the total probability per unit time at time t for one molecule of species l to jump from voxel $\boldsymbol{j}$ to voxel $\boldsymbol{i}$ is $k_{\boldsymbol{ij}}^l M_{\boldsymbol{j}}^l(t)$. $k_{\boldsymbol{ii}}^l$ is chosen to be zero, so that a molecule must hop to a different voxel.

We assume there are K possible reactions, with the function $a_{\boldsymbol{i}}^k(\boldsymbol{m_i})$ giving the probability per unit time of reaction k occurring in the $\boldsymbol{i}$th voxel when $\boldsymbol{M_i}(t) = \boldsymbol{m_i}$. For example, letting k label the unimolecular (first order) reaction $\mathrm{S}^l \rightarrow \mathrm{S}^{l'}$, then $a_{\boldsymbol{i}}^k(\boldsymbol{m_i}) = \alpha\, m_{\boldsymbol{i}}^l$, where α is the rate constant in units of number of occurrences of the reaction per molecule of S^l per unit time. Letting k' denote the index of the bimolecular reaction $\mathrm{S}^l + \mathrm{S}^{l'} \rightarrow \mathrm{S}^{l''}$, where $l \neq l'$, then $a_{\boldsymbol{i}}^{k'}(\boldsymbol{m_i}) = \beta\, m_{\boldsymbol{i}}^l m_{\boldsymbol{i}}^{l'}$. Here β is the rate constant in units of number of occurrences of the reaction per molecule of S^l and per molecule of $\mathrm{S}^{l'}$, per unit time. State changes in $\boldsymbol{M_i}(t)$ due to an occurrence of the kth chemical reaction in the $\boldsymbol{i}$th mesh voxel will be denoted by the vector $\boldsymbol{\nu}_k = (\nu_k^1, \ldots, \nu_k^L)$ (i.e., $\boldsymbol{M_i}(t) \rightarrow \boldsymbol{M_i}(t) + \boldsymbol{\nu}_k$). The corresponding state change in $\boldsymbol{M}(t)$ due to an occurrence of the kth reaction in the $\boldsymbol{i}$th voxel will be denoted by $\boldsymbol{\nu}_k\, 1_{\boldsymbol{i}}$ (i.e., $\boldsymbol{M}(t) \rightarrow \boldsymbol{M}(t) + \boldsymbol{\nu}_k\, 1_{\boldsymbol{i}}$). (Here $\boldsymbol{\nu}_k 1_{\boldsymbol{i}}$ is simply used as a notation to indicate that $\boldsymbol{M}(t)$ should change by $\boldsymbol{\nu}_k$ in the $\boldsymbol{i}$th voxel.)

With these definitions, the RDME for the time evolution of $P(\boldsymbol{m}, t)$ is then

$$\begin{aligned}\frac{dP(\boldsymbol{m},t)}{dt} = &\sum_{\boldsymbol{i}\in I}\sum_{\boldsymbol{j}\in I}\sum_{l=1}^{L}\left(k_{\boldsymbol{ij}}^l\left(m_{\boldsymbol{j}}^l+1\right)P(\boldsymbol{m}+1_{\boldsymbol{j}}^l-1_{\boldsymbol{i}}^l,t)-k_{\boldsymbol{ji}}^l m_{\boldsymbol{i}}^l P(\boldsymbol{m},t)\right)\\ &+\sum_{\boldsymbol{i}\in I}\sum_{k=1}^{K}\left(a_{\boldsymbol{i}}^k(\boldsymbol{m_i}-\boldsymbol{\nu}_k)P(\boldsymbol{m}-\boldsymbol{\nu}_k\,1_{\boldsymbol{i}},t)-a_{\boldsymbol{i}}^k(\boldsymbol{m_i})P(\boldsymbol{m},t)\right).\end{aligned} \tag{1.2}$$

This is a coupled set of ODEs over all possible nonnegative integer values of the matrix $\boldsymbol{m}$. Notice the important point that the reaction probabilities per unit time, $a_{\boldsymbol{i}}^k(\boldsymbol{m_i})$, may depend on spatial location. To the authors' knowledge, this equation goes back to the work of Gardiner [20].

Equation (1.2) is separated into two sums. The first term corresponds to diffusive motion between voxels $\boldsymbol{i}$ and $\boldsymbol{j}$ of a given species, l. The second is just the components of the chemical master equation [34], but applied at each individual voxel. In previous

work we have shown that, as the mesh spacing approaches zero, to recover diffusion of an individual molecule in a system with no chemical reactions or to recover diffusion of the mean chemical concentration of each species in (1.2), the diffusive jump rates should be chosen so as to determine a discretization of the Laplacian [28].

Let D^l denote the diffusion constant of chemical species l, specifically the macroscopic diffusion constant used in deterministic reaction-diffusion PDE models. (See section 1.1.3 for the relationship between the RDME and deterministic PDE models.) For a regular Cartesian mesh in $\mathbb{R}^d$ comprised of hypercubic voxels with width h, the diffusive jump rates for species l would be given by

$$k^l_{\boldsymbol{ji}} = \begin{cases} D^l/h^2, & \boldsymbol{i} \text{ a nondiagonal neighbor of } \boldsymbol{j}, \\ 0, & \text{otherwise.} \end{cases}$$

Denote by $\boldsymbol{e}_k$ the unit vector along the kth coordinate axis of $\mathbb{R}^d$. We define

$$\sum_{\pm}$$

to be the sum where every term is evaluated with any $\pm$ replaced by a $+$, and added to each term with any $\pm$ replaced by a $-$. As an example,

$$\sum_{\pm} \gamma_{\pm} = \gamma_+ + \gamma_-.$$

For a Cartesian mesh in $\mathbb{R}^d$ the RDME (1.2) then simplifies to

$$\begin{aligned} \frac{dP(\boldsymbol{m},t)}{dt} = &\sum_{\boldsymbol{i}\in\mathbb{Z}^d} \sum_{k=1}^{d} \sum_{\pm} \sum_{l=1}^{L} \frac{D^l}{h^2} \left(\left(m^l_{\boldsymbol{i}\pm\boldsymbol{e}_k} + 1 \right) P(\boldsymbol{m} + 1^l_{\boldsymbol{i}\pm\boldsymbol{e}_k} - 1^l_{\boldsymbol{i}}, t) - m^l_{\boldsymbol{i}} P(\boldsymbol{m},t) \right) \\ &+ \sum_{\boldsymbol{i}\in\mathbb{Z}^d} \sum_{k=1}^{K} \left(a^k_{\boldsymbol{i}}(\boldsymbol{m}_{\boldsymbol{i}} - \boldsymbol{\nu}_k) P(\boldsymbol{m} - \boldsymbol{\nu}_k\, 1_{\boldsymbol{i}}, t) - a^k_{\boldsymbol{i}}(\boldsymbol{m}_{\boldsymbol{i}}) P(\boldsymbol{m},t) \right). \end{aligned} \tag{1.3}$$

1.1.2. Physical validity. To date, no rigorous derivation of the RDME from a more microscopic physical model has been given. One systematic computational study was reported in [9] showing good agreement between the RDME and Boltzmann-like dynamics. The validity of the RDME model is often assumed based on the physical argument presented below (see, for example, the supplement to [15]).

First order reactions are assumed to represent internal events, and as such are presupposed to be independent of diffusion. We also assume that on relevant spatial scales of interest, molecular interaction forces are weak, so that until two molecules are sufficiently close they do not influence each other's movement. Motion of molecules is then taken to be purely diffusive. To ensure that the continuous-time random walk approximation to diffusion inherent in the RDME is accurate, we must choose the mesh spacing significantly smaller than characteristic length scales of interest. Denoting this length scale by L, and the width of a (cubic) voxel by h, we then require

$$L \gg h. \tag{1.4}$$

The primary physical assumption in formulating the RDME is that a separation of timescales exists such that on the spatial scale of voxels bimolecular reactions may

be treated as well mixed. For example, consider the bimolecular reaction $\mathrm{A} + \mathrm{B} \to \mathrm{C}$ with rate constant K. It is assumed that within a given voxel the timescale, τ_{K_A}, of a well-mixed bimolecular reaction between one specific molecule of chemical species A and any molecule of species B is much larger than the timescale, τ_D, for the A molecule and an arbitrary B molecule to become well-mixed relative to each other due to diffusion. (Here $D = D^\mathrm{A} + D^\mathrm{B}$ denotes the relative diffusion constant between the A and B molecules.) We specifically assume that

$$\tau_{K_\mathrm{A}} \gg \tau_D, \tag{1.5}$$

where

$$\tau_{K_\mathrm{A}} \approx \frac{1}{K\,[B]}, \qquad \tau_D \approx \frac{h^2}{D}.$$

Letting n_B denote the number of B molecules inside the voxel, then in three dimensions $[\mathrm{B}] = n_\mathrm{B}/h^3$, so that (1.5) simplifies to

$$h \gg \frac{K n_\mathrm{B}}{D}.$$

Combining this with (1.4), we have that

$$L \gg h \gg \frac{K n_\mathrm{B}}{D}. \tag{1.6}$$

It is therefore necessary to bound h from above and below to ensure accuracy of the RDME.

1.1.3. Relation to deterministic reaction-diffusion PDEs. We now examine the relation between the RDME and standard deterministic reaction-diffusion PDE models. Define $V_{\boldsymbol{i}}$ to be the volume of the $\boldsymbol{i}$th voxel. We let $C^l_{\boldsymbol{i}}(t) = M^l_{\boldsymbol{i}}(t)/V_{\boldsymbol{i}}$ be the random variable for the chemical concentration of species l, in voxel $\boldsymbol{i}$, and define $\boldsymbol{C}_{\boldsymbol{i}}(t) = (C^1_{\boldsymbol{i}}, \ldots, C^L_{\boldsymbol{i}})$. Denote by $\tilde{a}^k_{\boldsymbol{i}}$ the concentration dependent form of $a^k_{\boldsymbol{i}}$. $\tilde{a}^k_{\boldsymbol{i}}$ and $a^k_{\boldsymbol{i}}$ are related by $\tilde{a}^k_{\boldsymbol{i}}(\boldsymbol{c}) = a^k_{\boldsymbol{i}}(V_{\boldsymbol{i}}\boldsymbol{c})/V_{\boldsymbol{i}}$ and, vice versa, $a^k_{\boldsymbol{i}}(\boldsymbol{m}) = \tilde{a}^k_{\boldsymbol{i}}(\boldsymbol{m}/V_{\boldsymbol{i}})V_{\boldsymbol{i}}$. Letting $\mathbb{E}[C^l_{\boldsymbol{i}}(t)]$ denote the average value of $C^l_{\boldsymbol{i}}(t)$, from (1.2) we then find

$$\frac{d\,\mathbb{E}[C^l_{\boldsymbol{i}}]}{dt} = \sum_{\boldsymbol{j}\in I}\left(\frac{V_{\boldsymbol{j}}}{V_{\boldsymbol{i}}} k^l_{\boldsymbol{ij}}\,\mathbb{E}[C^l_{\boldsymbol{j}}] - k^l_{\boldsymbol{ji}}\,\mathbb{E}[C^l_{\boldsymbol{i}}]\right) + \sum_{k=1}^{K} \nu^l_k \mathbb{E}[\tilde{a}^k_{\boldsymbol{i}}\,(C_{\boldsymbol{i}})].$$

Note the important point that for nonlinear reactions, such as bimolecular reactions,

$$\mathbb{E}[\tilde{a}^k_{\boldsymbol{i}}\,(C_{\boldsymbol{i}}(t))] \neq \tilde{a}^k_{\boldsymbol{i}}\,(\mathbb{E}[C_{\boldsymbol{i}}(t)])\,. \tag{1.7}$$

For chemical systems in which any nonlinear reactions are present, the equations for the mean concentrations will then be coupled to an infinite set of ODEs for the higher order moments.

We now consider the continuum limit that $h \to 0$. Let $\boldsymbol{x}$ denote the centroid of the voxel labeled by $\boldsymbol{i}$, and assume that h is chosen to approach zero such that $\boldsymbol{x}$ always remains the centroid of some voxel. We then define

$$S^l(\boldsymbol{x}, t) = \lim_{h\to 0} \mathbb{E}[C^l_{\boldsymbol{i}}(t)]$$

and $\boldsymbol{S}(\boldsymbol{x},t) = (S^1(\boldsymbol{x},t),\ldots,S^L(\boldsymbol{x},t))$. Denote by D^l the diffusion constant of the lth chemical species, and define $\tilde{a}^k(\boldsymbol{S}(\boldsymbol{x},t),\boldsymbol{x})$ to be the continuum spatially varying concentration dependent form of $a^k_{\boldsymbol{i}}$. Following the discussion in subsection 1.1.1, the jump rates $k^l_{\boldsymbol{ij}}$ are chosen to be a discretization of the Laplacian. The deterministic reaction-diffusion PDE model can be thought of as the *approximation* that

$$\frac{\partial S^l(\boldsymbol{x},t)}{\partial t} = D^l \Delta S^l + \sum_{k=1}^{K} \nu^l_k \, \tilde{a}^k(\boldsymbol{S}(\boldsymbol{x},t),\boldsymbol{x}).$$

This equation implicitly assumes that in the formal continuum limit the equations for the mean concentrations form a closed system. In general, however, this is true only for chemical systems in which all reaction terms are linear due to (1.7). For systems with nonlinear reaction terms, the equations for the mean concentrations would then remain coupled to higher order moments in the formal continuum limit, giving an infinite system of equations to solve in order to determine the means.

As discussed in the introduction, it has been shown more generally that the formal continuum limit of the RDME itself may be interpreted as a Fock-space representation of a quantum field theory [39].

2. A reduced model to study h dependence of RDME. We now investigate the behavior of RDME as the mesh spacing, h, becomes small in a simplified model. The simplified model studied is that of two molecules, one of chemical species A and one of chemical species B, that diffuse in $\mathbb{R}^3$ and can be annihilated by undergoing the chemical reaction $\mathrm{A}+\mathrm{B} \to \varnothing$. In this system, the RDME can be reduced to a form that is much easier to study analytically than (1.3). (Note that we subsequently assume we are working in $\mathbb{R}^3$ with a standard cubic Cartesian mesh of mesh width h.) We show that in this special case the continuum limit is formally given by a PDE with distributional coefficients.

The model problem can be derived from the RDME (1.3) as follows. We first simplify to the reaction $\mathrm{A}+\mathrm{B} \to \mathrm{C}$ with well-mixed bimolecular reaction rate k, and only one molecule of A, one molecule of B, and no molecules of C initially. k is assumed to have units of volume/time as is standard for deterministic ODE models. We denote by $\boldsymbol{A}(t) = \{A_{\boldsymbol{i}}(t)\}_{\boldsymbol{i}\in\mathbb{Z}^3}$ the vector stochastic process for the number of molecules of chemical species A at each location at time t. (We define $\boldsymbol{B}(t)$ and $\boldsymbol{C}(t)$ similarly.) $a_{\boldsymbol{i}}$ will denote a specific number of molecules of chemical species A at location $\boldsymbol{i}$, and

$$\boldsymbol{a} = \{a_{\boldsymbol{i}} \mid \boldsymbol{i} \in \mathbb{Z}^3\},$$

a possible value of $\boldsymbol{A}(t)$. (We again define $\boldsymbol{b}$ and $\boldsymbol{c}$ similarly.) The notation $\boldsymbol{a}+1_{\boldsymbol{i}}$ will, as before, represent $\boldsymbol{a}$ with one added to $a_{\boldsymbol{i}}$. In terms of $\boldsymbol{a}$, $\boldsymbol{b}$, and $\boldsymbol{c}$, the RDME gives the time evolution of

$$P(\boldsymbol{a},\boldsymbol{b},\boldsymbol{c},t) = \mathrm{Prob}\left\{\boldsymbol{A}(t)=\boldsymbol{a},\boldsymbol{B}(t)=\boldsymbol{b},\boldsymbol{C}(t)=\boldsymbol{c} \mid \boldsymbol{A}(0),\boldsymbol{B}(0),\boldsymbol{C}(0)\right\}.$$

Let $\boldsymbol{0}$ denote the zero vector. We assume that $\boldsymbol{A}(0) = 1_{\boldsymbol{i}_0}$, $\boldsymbol{B}(0) = 1_{\boldsymbol{i}'_0}$, and $\boldsymbol{C}(0) = \boldsymbol{0}$. At time t, the state of the chemical system is then $\boldsymbol{A}(t) = 1_{\boldsymbol{i}}$, $\boldsymbol{B}(t) = 1_{\boldsymbol{i}'}$, and $\boldsymbol{C}(t) = \boldsymbol{0}$ prior to the reaction occurring, or $\boldsymbol{A}(t) = \boldsymbol{0}$, $\boldsymbol{B}(t) = \boldsymbol{0}$, and $\boldsymbol{C}(t) = 1_{\boldsymbol{i}}$ subsequent to the reaction occurring. (Here $\boldsymbol{i}$ and $\boldsymbol{i}'$ label arbitrary molecule positions.) Let $\delta_{\boldsymbol{i}\boldsymbol{i}'}$ denote the three-dimensional Kronecker delta function, zero if $\boldsymbol{i} \neq \boldsymbol{i}'$ and one if $\boldsymbol{i} = \boldsymbol{i}'$.

For this system, the RDME (1.3) simplifies to

$$\frac{dP}{dt}(1_{\boldsymbol{i}},1_{\boldsymbol{i}'},\mathbf{0}) = \sum_{k=1}^{3}\sum_{\pm}\Big[\frac{D^{\mathrm{A}}}{h^2}\big(P(1_{\boldsymbol{i}\pm\boldsymbol{e}_k},1_{\boldsymbol{i}'},\mathbf{0},t)-P(1_{\boldsymbol{i}},1_{\boldsymbol{i}'},\mathbf{0},t)\big) + \frac{D^{\mathrm{B}}}{h^2}\big(P(1_{\boldsymbol{i}},1_{\boldsymbol{i}'\pm\boldsymbol{e}_k},\mathbf{0},t)-P(1_{\boldsymbol{i}},1_{\boldsymbol{i}'},\mathbf{0},t)\big)\Big] - \frac{k}{h^3}\delta_{\boldsymbol{i}\boldsymbol{i}'}P(1_{\boldsymbol{i}},1_{\boldsymbol{i}'},\mathbf{0},t)$$

for states where a reaction has not yet occurred, and to

$$\frac{dP}{dt}(\mathbf{0},\mathbf{0},1_{\boldsymbol{i}}) = \sum_{k=1}^{3}\sum_{\pm}\frac{D^{\mathrm{C}}}{h^2}\big[P(\mathbf{0},\mathbf{0},1_{\boldsymbol{i}\pm\boldsymbol{e}_k},t)-P(\mathbf{0},\mathbf{0},1_{\boldsymbol{i}},t)\big]+\frac{k}{h^3}P(1_{\boldsymbol{i}},1_{\boldsymbol{i}},\mathbf{0},t)$$

for states where the reaction has occurred. Note the important point that the bimolecular reaction rate is given by k/h^3, since k has units of volume/time.

This simplified RDME is completely equivalent to a new representation described by the probability distributions $F^{(0,0,1)}(\boldsymbol{i},t)$ and $F^{(1,1,0)}(\boldsymbol{i},\boldsymbol{i}',t)$. Here superscripts denote the total number of each of species A, B, and C in the system, and indices give the corresponding locations of these molecules. $F^{(1,1,0)}(\boldsymbol{i},\boldsymbol{i}',t)$ denotes the probability that the species A and B particles have not yet reacted and are located in voxels $\boldsymbol{i}$ and $\boldsymbol{i}'$, respectively, at time t. $F^{(0,0,1)}(\boldsymbol{i},t)$ gives the probability that the particles have reacted and that the C particle they created is located in voxel $\boldsymbol{i}$ at time t.

Assuming that the A particle starts in voxel $\boldsymbol{i}_0$ and the B particle in voxel $\boldsymbol{i}'_0$, the equations of evolution of $F^{(0,0,1)}(\boldsymbol{i},t)$ and $F^{(1,1,0)}(\boldsymbol{i},\boldsymbol{i}',t)$ follow immediately from the simplified RDME, and are given by

(2.1)
$$\frac{dF^{(1,1,0)}}{dt}(\boldsymbol{i},\boldsymbol{i}',t) = \left(\left[D^{\mathrm{A}}\Delta_h^{\mathrm{A}}+D^{\mathrm{B}}\Delta_h^{\mathrm{B}}\right]F^{(1,1,0)}\right)(\boldsymbol{i},\boldsymbol{i}',t)-\frac{k}{h^3}\delta_{\boldsymbol{i}\boldsymbol{i}'}F^{(1,1,0)}(\boldsymbol{i},\boldsymbol{i},t),$$

(2.2)
$$\frac{dF^{(0,0,1)}}{dt}(\boldsymbol{i},t) = \left(D^{\mathrm{C}}\Delta_h^{\mathrm{C}}F^{(0,0,1)}\right)(\boldsymbol{i},t)+\frac{k}{h^3}F^{(1,1,0)}(\boldsymbol{i},\boldsymbol{i},t),$$

with initial conditions $F^{(1,1,0)}(\boldsymbol{i},\boldsymbol{i}',0)=\delta_{\boldsymbol{i}\boldsymbol{i}_0}\delta_{\boldsymbol{i}'\boldsymbol{i}'_0}$ and $F^{(0,0,1)}(\boldsymbol{i},0)=0$. Here Δ_h^{A} denotes the standard second order discrete Laplacian acting on the coordinates of the A particle, and Δ_h^{B} denotes the discrete Laplacian acting on the coordinates of the species B particle. For example,

$$\left(\Delta_h^{\mathrm{B}}F^{(1,1,0)}\right)(\boldsymbol{i},\boldsymbol{i}',t)=\sum_{k=1}^{3}\sum_{\pm}\frac{1}{h^2}\left(F^{(1,1,0)}(\boldsymbol{i},\boldsymbol{i}'\pm\boldsymbol{e}_k,t)-F^{(1,1,0)}(\boldsymbol{i},\boldsymbol{i}',t)\right).$$

Δ_h^{C} is defined similarly. More general multiparticle RDMEs can also be converted to related systems of coupled differential-difference equations. These equations correspond to discrete versions of the spatially continuous "distribution function" stochastic reaction-diffusion model proposed in [14]. Note that if the number of reacting molecules is unbounded, the number of equations will be infinite. See [26] for a derivation of the corresponding system of equations governing the reaction $\mathrm{A}+\mathrm{B}\leftrightarrows\mathrm{C}$ with arbitrary amounts of each chemical species.

Notice that (2.1) is independent of (2.2), and by itself can be thought of as representing the reaction $\mathrm{A}+\mathrm{B}\to\varnothing$. To study this chemical reaction we drop the C dependence in $F^{(1,1,0)}(\boldsymbol{i},\boldsymbol{i}',t)$ and study $F^{(1,1)}(\boldsymbol{i},\boldsymbol{i}',t)$, which satisfies

$$\frac{dF^{(1,1)}}{dt}(\boldsymbol{i},\boldsymbol{i}',t)=\left(\left[D^{\mathrm{A}}\Delta_h^{\mathrm{A}}+D^{\mathrm{B}}\Delta_h^{\mathrm{B}}\right]F^{(1,1)}\right)(\boldsymbol{i},\boldsymbol{i}',t)-\frac{k}{h^3}\delta_{\boldsymbol{i}\boldsymbol{i}'}F^{(1,1)}(\boldsymbol{i},\boldsymbol{i},t), \tag{2.3}$$

with initial condition $F^{(1,1)}(\boldsymbol{i},\boldsymbol{i}',0)=\delta_{\boldsymbol{i}\boldsymbol{i}_0}\delta_{\boldsymbol{i}'\boldsymbol{i}'_0}$.

We now consider the separation vector, $\boldsymbol{i}-\boldsymbol{i}'$, for the two particles of species A and B. Define the probability of the separation vector having the value $\boldsymbol{j}$,

$$\begin{aligned}P(\boldsymbol{j},t)&=\sum_{\boldsymbol{i}-\boldsymbol{i}'=\boldsymbol{j}}F^{(1,1)}(\boldsymbol{i},\boldsymbol{i}',t)\\&=\sum_{\boldsymbol{i}\in Z^3}F^{(1,1)}(\boldsymbol{i},\boldsymbol{i}-\boldsymbol{j},t).\end{aligned} \tag{2.4}$$

It follows from (2.3), as shown in [25], that $P(\boldsymbol{j},t)$ satisfies

$$\begin{aligned}\frac{dP}{dt}(\boldsymbol{j},t)&=(D\Delta_hP)(\boldsymbol{j},t)-\frac{k}{h^3}\delta_{\boldsymbol{j}\boldsymbol{0}}P(\boldsymbol{0},t),\\P(\boldsymbol{j},0)&=\delta_{\boldsymbol{j}\boldsymbol{j}_0},\end{aligned} \tag{2.5}$$

where Δ_h is acting on the $\boldsymbol{j}$ index, $D=D^{\mathrm{A}}+D^{\mathrm{B}}$, and $\boldsymbol{j}_0=\boldsymbol{i}_0-\boldsymbol{i}'_0$. Note that this equation is equivalent to an RDME model of the binding of a *single* diffusing particle to a *fixed* binding site at the origin.

To study the limiting behavior of our system for small h we convert (2.5) from units of probability to units of probability density. This change is necessary since the underlying SCDLR model we compare with is described by the evolution of a probability density. Let $\boldsymbol{x}_{\boldsymbol{j}}=h\boldsymbol{j}$ denote the center of the Cartesian voxel labeled by $\boldsymbol{j}\in\mathbb{Z}^3$. We denote the probability density for the separation vector to be $\boldsymbol{x}_{\boldsymbol{j}}$ at time t by $p_h(\boldsymbol{x}_{\boldsymbol{j}},t)\equiv P(\boldsymbol{j},t)/h^3$. Equation (2.5) can now be converted to an equation for $p_h(\boldsymbol{x}_{\boldsymbol{j}},t)$, giving

$$\begin{aligned}\frac{dp_h}{dt}(\boldsymbol{x}_{\boldsymbol{j}},t)&=D(\Delta_hp_h)(\boldsymbol{x}_{\boldsymbol{j}},t)-\frac{k}{h^3}\delta_{\boldsymbol{j}\boldsymbol{0}}\,p_h(\boldsymbol{0},t),\\p_h(\boldsymbol{x}_{\boldsymbol{j}},0)&=\frac{1}{h^3}\delta_{\boldsymbol{j}\boldsymbol{j}_0},\quad \boldsymbol{j}_0\neq\boldsymbol{0},\end{aligned} \tag{2.6}$$

where again $\boldsymbol{j}_0=\boldsymbol{i}_0-\boldsymbol{i}'_0$. Note the assumption, which we use for the remainder of this paper, that initially the molecules are in different voxels, i.e., $\boldsymbol{j}_0\neq\boldsymbol{0}$. This assumption is necessary to avoid a product of delta functions centered at the same location in the SCDLR model used in section 2.2. Equation (2.6) is the final reduced form of the reaction $\mathrm{A}+\mathrm{B}\to\varnothing$ that we subsequently study.

In section 2.1 we consider the limit of this model as $h\to 0$ and observe that the molecules never react. In contrast, we show in section 2.2 that this simplified model can be thought of as a good asymptotic approximation to a specific microscopic continuous-space reaction-diffusion model, assuming that h is neither too small nor too large. Specifically, we show that the simplified discrete model can be thought of as an asymptotic approximation to an SCDLR model, where reactions are modeled as occurring instantly when two diffusing particles approach within a specified reaction-radius. The asymptotic approximation of (2.6) to the SCDLR model diverges like $1/h$

as $h \to 0$, and therefore the master equation loses accuracy when h is sufficiently small. Recall, however, that h cannot be taken arbitrarily large, as then neither diffusion nor the reaction process would be approximated accurately! In section 2.2.3 we investigate the error between the asymptotic approximations, truncated after the second order terms, of the SCDLR model and the simplified RDME model. Both numerically calculated error values and analytical convergence/divergence rates are presented. It is shown that for this simplified model the physically derived bounds on h given in section 1.1.2 may be reasonable restrictions on how h should be chosen so that the truncated asymptotic expansion of the RDME provides an accurate approximation to the truncated expansion of the SCDLR model.

2.1. Continuum limit as $h \to 0$. Let $\delta(\boldsymbol{x})$ denote the Dirac delta function. We might expect the solution to (2.6) to approach the solution to

$$\begin{aligned} \frac{\partial p}{\partial t}(\boldsymbol{x},t) &= D\Delta p(\boldsymbol{x},t) - k\delta(\boldsymbol{x})p(\boldsymbol{0},t), \quad \boldsymbol{x} \in \mathbb{R}^3, \\ p(\boldsymbol{x},0) &= \delta(\boldsymbol{x}-\boldsymbol{x}_0), \quad \boldsymbol{x}_0 \neq \boldsymbol{0}, \end{aligned} \tag{2.7}$$

as $h \to 0$. Ignoring, for now, the question of how to define a PDE with distributional coefficients, we next show that, as $h \to 0$, the molecules never react and simply diffuse relative to each other. Thus, in the continuum limit, the molecules do not feel the delta function reaction term at all.

To study the solution to (2.6) as $h \to 0$ we will make use of the free space Green's function for the discrete-space continuous-time diffusion equation, $G_h(\boldsymbol{x_j},t)$. G_h satisfies

$$\begin{aligned} \frac{dG_h}{dt}(\boldsymbol{x_j},t) &= D(\Delta_h G_h)(\boldsymbol{x_j},t), \\ G_h(\boldsymbol{x_j},0) &= \frac{1}{h^3}\delta_{\boldsymbol{j0}} \end{aligned} \tag{2.8}$$

and has the Fourier representation

$$G_h(\boldsymbol{x_j},t) = \iiint_{\left[\frac{-1}{2h},\frac{1}{2h}\right]^3} e^{-4Dt\sum_{k=1}^3 \sin^2(\pi h\xi_k)/h^2}\, e^{2\pi i\boldsymbol{\xi}\cdot(\boldsymbol{x_j})}\, d\boldsymbol{\xi}. \tag{2.9}$$

Here $\boldsymbol{\xi} = (\xi_1,\xi_2,\xi_3)$, and $[-1/2h, 1/2h]^3$ denotes the cube centered at the origin with sides of length $1/h$. We will also need the Green's function for the continuum free space diffusion equation, $G(\boldsymbol{x},t)$, given by

$$G(\boldsymbol{x},t) = \frac{1}{(4\pi Dt)^{3/2}} e^{-|\boldsymbol{x}|^2/(4Dt)}. \tag{2.10}$$

Note that we prove in Theorem B.1 that, away from the origin, G_h converges to G uniformly in time as $h \to 0$.

Using Duhamel's principle, the solution to (2.6) may be written as

$$p_h(\boldsymbol{x_j},t) = G_h(\boldsymbol{x_j}-\boldsymbol{x_{j_0}},t) - k\int_0^t G_h(\boldsymbol{x_j},t-s)p_h(\boldsymbol{0},s)\,ds. \tag{2.11}$$

Letting $\boldsymbol{x_j} = 0$, we find that the solution at the origin satisfies the Volterra integral equation of the second kind,

$$p_h(\boldsymbol{0},t) = G_h(\boldsymbol{x_{j_0}},t) - k\int_0^t G_h(\boldsymbol{0},t-s)p_h(\boldsymbol{0},s)\,ds, \tag{2.12}$$

where we have used that $G_h(\boldsymbol{x}_{\boldsymbol{j}} - \boldsymbol{x}_{\boldsymbol{j}_0}, t) = G_h(\boldsymbol{x}_{\boldsymbol{j}_0} - \boldsymbol{x}_{\boldsymbol{j}}, t)$. In Appendix A we prove that $p_h(\boldsymbol{x}_{\boldsymbol{j}}, t)$ is positive for all $\boldsymbol{j} \in \mathbb{Z}^3$ and $t > 0$, and for each fixed $\boldsymbol{x}_{\boldsymbol{j}}$ is continuous in t for all $t \in \mathbb{R}$.

We will also find it useful to consider the binding time distribution, $F_h(t)$, for the particles. Denote by T the random variable for the binding time of the particles; then $F_h(t) = \text{Prob}\{T < t\}$ and is given by

$$\begin{aligned} F_h(t) &\equiv k \int_0^t p_h(\mathbf{0}, s)\, ds \\ &= \frac{k}{h^3} \int_0^t P(\mathbf{0}, s)\, ds. \end{aligned} \tag{2.13}$$

Note that $F_h(t)$ may be defective, i.e., $F_h(\infty) < 1$, since in three dimensions the particle separation is not guaranteed to ever take the value $\mathbf{0}$ as $t \to \infty$. Considering the coupled system for both p_h and F_h, total probability is now conserved, so that

$$\sum_{\boldsymbol{j} \in \mathbb{Z}^3} \left(p_h(\boldsymbol{x}_{\boldsymbol{j}}, t) h^3 \right) + F_h(t) = 1 \quad \forall\, t \geq 0.$$

That $F_h(t)$ is a rigorously defined (possibly defective) probability distribution, and the validity of the preceding formula, are both proven in Appendix A.

For the remainder of this section we assume that $\boldsymbol{x} = \boldsymbol{x}_{\boldsymbol{j}} = h\boldsymbol{j}$ for some $\boldsymbol{j} \in \mathbb{Z}^3$ and remains fixed as $h \to 0$. (That is, we choose $\boldsymbol{j} = \boldsymbol{j}(h) \to \infty$ as $h \to 0$ such that $\boldsymbol{x} = h\boldsymbol{j}$ remains fixed.) We likewise assume that $\boldsymbol{x}_0 = \boldsymbol{x}_{\boldsymbol{j}_0} = h\boldsymbol{j}_0$ for some $\boldsymbol{j}_0 \in \mathbb{Z}^3$ and is also held fixed as $h \to 0$. With the preceding definitions, we now show that reaction effects are lost as $h \to 0$.

THEOREM 2.1. *Assume the initial particle separation $\boldsymbol{x}_0 \neq \mathbf{0}$ and is held fixed as $h \to 0$. For all $t \geq 0$, the probability that the particles have reacted by time t approaches zero as $h \to 0$; i.e.,*

$$\lim_{h \to 0} F_h(t) = 0. \tag{2.14}$$

In addition, assume that $\boldsymbol{x} \neq \mathbf{0}$ and is held fixed as $h \to 0$. Then for all $t > 0$ the solution to (2.11) *converges to the solution to the free space diffusion equation, i.e.,*

$$\lim_{h \to 0} p_h(\boldsymbol{x}, t) = G\left(\boldsymbol{x} - \boldsymbol{x}_0, t\right) \quad \forall\, t > 0. \tag{2.15}$$

As pointed out by a reviewer, since $F_h(t)$ is a (possibly defective) probability distribution, we in fact have uniform convergence of $F_h(t)$ to zero on any interval, $[0, T]$, with $T < \infty$.

Theorem 2.1 implies that, in the continuum limit, the particles never react and simply diffuse relative to each other. Figure 2.1 shows solution curves as h is varied, for $p_h(\mathbf{0}, t)$ in Figure 2.1(a) and for $p_h(\boldsymbol{x}, t)$ in Figure 2.1(b). A stronger result than the theorem is illustrated in Figure 2.2, where the numerical convergence of $p_h(\mathbf{0}, t)$ to zero and $p_h(\boldsymbol{x}, t)$ to $G(\boldsymbol{x} - \boldsymbol{x}_0, t)$ are illustrated as functions of h. We were unable to calculate $p_h(\mathbf{0}, t)$ for sufficiently small mesh widths, h, to resolve the asymptotic convergence rate of $p_h(\mathbf{0}, t)$ to zero, but the figure shows the decrease in $p_h(\mathbf{0}, t)$ as h is decreased. An apparent second order convergence rate of $p_h(\boldsymbol{x}, t)$ to $G(\boldsymbol{x} - \boldsymbol{x}_0, t)$ is also seen, though this convergence rate may not be the correct asymptotic rate (since to calculate $p_h(\boldsymbol{x}, t)$ we make use of $p_h(\mathbf{0}, t)$ through (2.11)). Details of the numerical methods used to find $p_h(\mathbf{0}, t)$ and $p_h(\boldsymbol{x}, t)$ may be found in Appendix C.

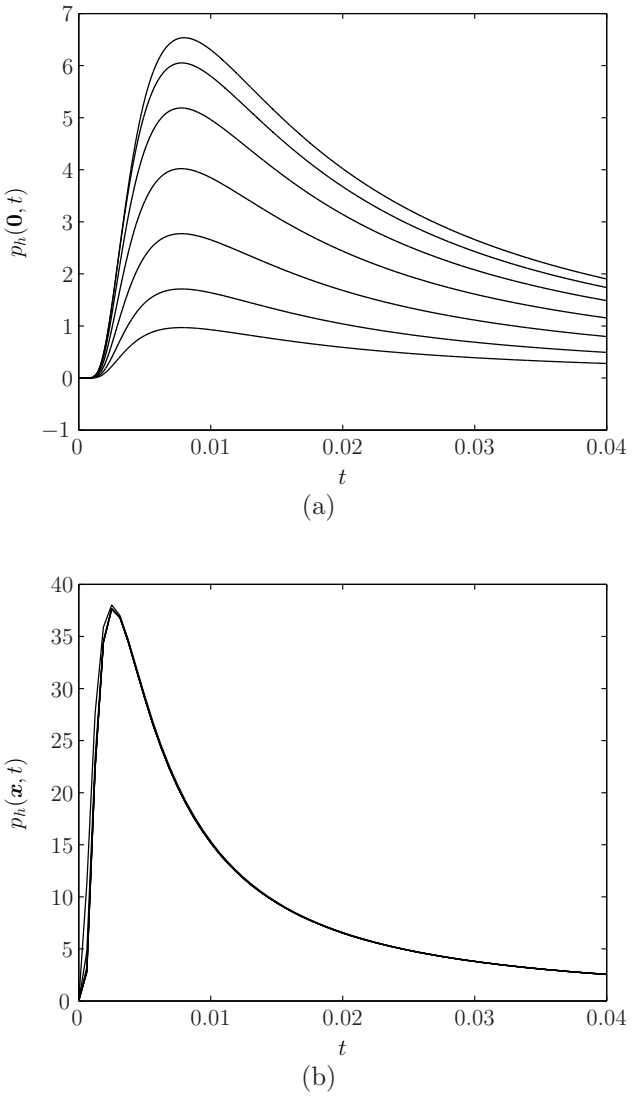

FIG. 2.1. (a) $p_h(0,t)$ *versus* t *on* $[0,.04]$. *Each curve on the figure corresponds to* $p_h(0,t)$ *for a different value of* h. *The topmost curve corresponds to* $h = 2^{-5}$, *the next largest to* 2^{-6}, *and so on through the bottom curve, corresponding to* $h = 2^{-11}$. (b) $p_h(\boldsymbol{x},t)$ *versus* t *on* $[0,.04]$ *at* $\boldsymbol{x} = (0,1/8,1/8)$. *Again curves are plotted for* $h = 2^{-5}$, 2^{-6}, $\ldots$, 2^{-11}; *however, they are visually indistinguishable. In both figures,* $\boldsymbol{x}_0 = (1/8,1/8,1/8)$, $D = 1$, *and* $k = 4\pi Da$, *where* $a = .001$.

To prove Theorem 2.1 we need the following two lemmas and Theorem B.1, which proves that away from the origin G_h converges to G uniformly in t as $h \to 0$.

LEMMA 2.2. *Assume* $\boldsymbol{x} \neq \mathbf{0}$ *and that* $\boldsymbol{x}$ *is fixed as* h *varies. Then for all* $\epsilon > 0$ *there exists an* $h_0 > 0$ *such that, for all* $h \leq h_0$,

$$G_h(\boldsymbol{x},t) \leq G(\boldsymbol{x},t) + \epsilon.$$

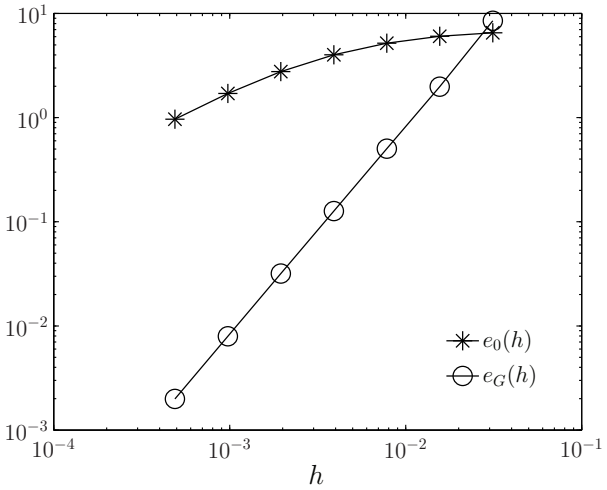

FIG. 2.2. *Convergence of $p_h(\mathbf{0},t)$ to zero and $p_h(\boldsymbol{x},t)$ to $G(\boldsymbol{x}-\boldsymbol{x}_0,t)$ as $h \to 0$. $e_0(h) = \max_{t\in[0,.04]} p_h(\mathbf{0},t)$, and $e_G(h) = \max_{t\in[0,.04]} |p_h(\boldsymbol{x},t) - G(\boldsymbol{x}-\boldsymbol{x}_0,t)|$. Note that the slope of the best fit line to $e_G(h) = 2.0035$. Values of $\boldsymbol{x}$, $\boldsymbol{x}_0$, D, and k are the same as in Figure* 2.1.

Moreover, for $h \le h_0$,

$$\sup_{t\ge 0} G_h(\boldsymbol{x},t) \le C,$$

where C is a constant depending only on $\boldsymbol{x}$ (independent of h and t).

Proof. In Theorem B.1 we prove that $G_h(\boldsymbol{x},t) \to G(\boldsymbol{x},t)$ uniformly in t. Hence for all $\epsilon > 0$ we can find an $h_0 > 0$ such that, for all $h \le h_0$,

$$G_h(\boldsymbol{x},t) \le G(\boldsymbol{x},t) + \epsilon.$$

$G(\boldsymbol{x},t)$ is maximized for $t = |\boldsymbol{x}|^2/6D$, so that

$$\sup_{t\ge 0} G_h(\boldsymbol{x},t) \le \left(\frac{3}{2\pi}\right)^{\frac{3}{2}} \frac{1}{|\boldsymbol{x}|^3}\, e^{-3/2} + \epsilon. \qquad \square$$

We will subsequently make use of the Laplace transform, defined for a function $f(t)$ as

$$\tilde{f}(s) = \int_0^\infty f(t) e^{-st}\, dt.$$

The second lemma we need is the following.

LEMMA 2.3. *Denote by $\tilde{G}_h(\boldsymbol{x},s)$ the Laplace transform of $G_h(\boldsymbol{x},t)$ with respect to t. We again assume that $\boldsymbol{x} \neq \mathbf{0}$ and that $\boldsymbol{x}$ is fixed as $h \to 0$. Then*

$$\lim_{h\to 0} \tilde{G}_h(\boldsymbol{x},s) = \tilde{G}(\boldsymbol{x},s) \quad \forall s > 0 \tag{2.16}$$

and

$$\lim_{h\to 0} \tilde{G}_h(\mathbf{0},s) = \infty \quad \forall s > 0. \tag{2.17}$$

Proof. By Theorem B.1, for each fixed $s > 0$, $G_h(\boldsymbol{x},t)e^{-st}$ converges uniformly in t to $G(\boldsymbol{x},t)e^{-st}$ as $h \to 0$. We may thus conclude that

$$\lim_{h\to 0}\int_0^\infty G_h(\boldsymbol{x},t)e^{-st}\,dt = \int_0^\infty G(\boldsymbol{x},t)e^{-st}\,dt.$$

By definition, this implies that $\tilde{G}_h(\boldsymbol{x},s) \to \tilde{G}(\boldsymbol{x},s)$ for all $s > 0$ as $h \to 0$.

For the second limit, we have that, for all $t > 0$, $G_h(\mathbf{0},t) \to G(0,t) = 1/(4\pi Dt)^{3/2}$ as $h \to 0$ by Theorem B.1. Therefore, by Fatou's lemma,

$$\begin{aligned}\liminf_{h\to 0}\int_0^\infty G_h(\mathbf{0},t)e^{-st}\,dt &\geq \int_0^\infty \liminf_{h\to 0} G_h(\mathbf{0},t)e^{-st}\,dt\\ &= \int_0^\infty \frac{1}{(4\pi Dt)^{3/2}}e^{-st}\,dt\\ &= \infty. \qquad \square\end{aligned}$$

With these lemmas, we may now prove the main theorem of this section.

Proof of Theorem 2.1. Taking the Laplace transform of (2.12), we find

$$\tilde{p}_h(\mathbf{0},s) = \frac{\tilde{G}_h(\boldsymbol{x}_0,s)}{1 + k\tilde{G}_h(\mathbf{0},s)}.$$

Lemma 2.3 then implies

$$\lim_{h\to 0}\tilde{p}_h(\mathbf{0},s) = 0 \quad \forall s > 0.$$

By (2.13), $k\,p_h(\mathbf{0},t)$ is the binding time density corresponding to the binding time distribution, $F_h(t)$. Since $k\tilde{p}_h(\mathbf{0},s) \to 0$ as $h \to 0$, the continuity theorem [18, section XIII.2, Theorem 2a] implies that

$$\lim_{h\to 0} F_h(t) = 0.$$

Equation (2.11) implies

$$|p_h(\boldsymbol{x},t) - G_h(\boldsymbol{x}-\boldsymbol{x}_0,t)| \leq k\int_0^t G_h(\boldsymbol{x},t-s)p_h(\mathbf{0},s)\,ds.$$

For all h sufficiently small, Lemma 2.2 implies

$$\begin{aligned}|p_h(\boldsymbol{x},t) - G_h(\boldsymbol{x}-\boldsymbol{x}_0,t)| &\leq k\left(\sup_t G(\boldsymbol{x},t) + \epsilon\right)\int_0^t p_h(\mathbf{0},s)\,ds\\ &= \left(\sup_t G(\boldsymbol{x},t) + \epsilon\right)F_h(t).\end{aligned}$$

$F_h(t)$ goes to zero and $G_h(\boldsymbol{x}-\boldsymbol{x}_0,t) \to G(\boldsymbol{x}-\boldsymbol{x}_0,t)$ as $h \to 0$ by Theorem B.1, so that we may conclude $p_h(\boldsymbol{x},t) \to G(\boldsymbol{x}-\boldsymbol{x}_0,t)$ as $h \to 0$. $\square$

2.2. RDME as an asymptotic approximation of diffusion to a small target. While reaction effects are lost as $h \to 0$, we will now show that for h small, but not "too" small, the simplified model given by (2.5) provides an approximation to an SCDLR model. We consider a system consisting of two diffusing molecules, one

of species A and one of species B. The reaction $\mathrm{A}+\mathrm{B}\to\varnothing$ is modeled by having the two molecules be annihilated instantly when they reach a certain physical separation length, called the reaction-radius and denoted by a. We define $f^{(1,1)}(\boldsymbol{q}^{\mathrm{A}},\boldsymbol{q}^{\mathrm{B}},t)$ to represent the probability density for both molecules to exist, the A molecule to be at $\boldsymbol{q}^{\mathrm{A}}$, and the B molecule to be at $\boldsymbol{q}^{\mathrm{B}}$ at time t. The model is then

(2.18)
$$\begin{aligned}
\frac{\partial f^{(1,1)}}{\partial t}(\boldsymbol{q}^{\mathrm{A}},\boldsymbol{q}^{\mathrm{B}},t) &= \left(\left[D^{\mathrm{A}}\Delta^{\mathrm{A}}+D^{\mathrm{B}}\Delta^{\mathrm{B}}\right]f^{(1,1)}\right)(\boldsymbol{q}^{\mathrm{A}},\boldsymbol{q}^{\mathrm{B}},t), \quad && \left|\boldsymbol{q}^{\mathrm{A}}-\boldsymbol{q}^{\mathrm{B}}\right|>a,\\
f^{(1,1)}(\boldsymbol{q}^{\mathrm{A}},\boldsymbol{q}^{\mathrm{B}},t) &= 0, && \left|\boldsymbol{q}^{\mathrm{A}}-\boldsymbol{q}^{\mathrm{B}}\right|=a,\\
\lim_{|\boldsymbol{q}^{\mathrm{A}}|\to\infty} f^{(1,1)}(\boldsymbol{q}^{\mathrm{A}},\boldsymbol{q}^{\mathrm{B}},t) &= 0,\\
\lim_{|\boldsymbol{q}^{\mathrm{B}}|\to\infty} f^{(1,1)}(\boldsymbol{q}^{\mathrm{A}},\boldsymbol{q}^{\mathrm{B}},t) &= 0,\\
f^{(1,1)}(\boldsymbol{q}^{\mathrm{A}},\boldsymbol{q}^{\mathrm{B}},0) &= \delta(\boldsymbol{q}^{\mathrm{A}}-\boldsymbol{q}_0^{\mathrm{A}})\delta(\boldsymbol{q}^{\mathrm{B}}-\boldsymbol{q}_0^{\mathrm{B}}), && \boldsymbol{q}_0^{\mathrm{A}}\neq\boldsymbol{q}_0^{\mathrm{B}}.
\end{aligned}$$

For simplicity, we again convert to the system for the separation vector, $\boldsymbol{x}=\boldsymbol{q}^{\mathrm{A}}-\boldsymbol{q}^{\mathrm{B}}$, between the A and B particles. Let $p(\boldsymbol{x},t)$ represent the probability density that the particles have the separation vector $\boldsymbol{x}$ at time t. $p(\boldsymbol{x},t)$ then satisfies

(2.19)
$$\begin{aligned}
\frac{\partial p}{\partial t}(\boldsymbol{x},t) &= D\Delta p(\boldsymbol{x},t), \quad && |\boldsymbol{x}|>a,\\
p(\boldsymbol{x},t) &= 0, && |\boldsymbol{x}|=a,\\
\lim_{|\boldsymbol{x}|\to\infty} p(\boldsymbol{x},t) &= 0,\\
p(\boldsymbol{x},0) &= \delta(\boldsymbol{x}-\boldsymbol{x}_0), \quad && \boldsymbol{x}_0\neq\mathbf{0},
\end{aligned}$$

where $D=D^{\mathrm{A}}+D^{\mathrm{B}}$ and $\boldsymbol{x}_0=\boldsymbol{q}_0^{\mathrm{A}}-\boldsymbol{q}_0^{\mathrm{B}}$. We subsequently refer to (2.19) as the SCDLR model.

Recall the definition of $p_h(\boldsymbol{x}_{\boldsymbol{j}},t)$, the probability density for the particle separation from the master equation to be $\boldsymbol{x}_{\boldsymbol{j}}$ at time t; see (2.6) (where $\boldsymbol{x}_{\boldsymbol{j}}=h\boldsymbol{j}$, $\boldsymbol{j}\in\mathbb{Z}^3$). We expect that $p_h(\boldsymbol{x}_{\boldsymbol{j}},t)\approx p(\boldsymbol{x}_{\boldsymbol{j}},t)$ for h small but not "too small."

Our main assumption is that $h\gg a$, motivated by the simplification of the heuristic physical assumption, (1.6), in the case of one particle of chemical species A and one particle of chemical species B,

$$h\gg\frac{k}{D}.$$

We relate the reaction-radius, a, to k/D through the *definition*

$$a=\frac{k}{4\pi D}.$$

This definition agrees with the well-known form of the bimolecular reaction rate constant for a strongly diffusion limited reaction (see, for example, [29] for a review of the relevant theory and [43] for the original work). Our key assumption is that k/D is a small parameter, relative to spatial scales of interest, that determines the size of the reaction-radius in (2.19).

Replacing k with $4\pi Da$, (2.6) becomes

(2.20)
$$\begin{aligned}
\frac{dp_h}{dt}(\boldsymbol{x}_{\boldsymbol{j}},t) &= D(\Delta_h p_h)(\boldsymbol{x}_{\boldsymbol{j}},t)-\frac{4\pi Da}{h^3}\delta_{\boldsymbol{j}\mathbf{0}}\,p_h(\mathbf{0},t),\\
p_h(\boldsymbol{x}_{\boldsymbol{j}},0) &= \frac{1}{h^3}\delta_{\boldsymbol{j}\boldsymbol{j}_0},
\end{aligned}$$

where again $\boldsymbol{j}_0 = \boldsymbol{i}_0 - \boldsymbol{i}'_0$. It is this equation we compare to the SCDLR model, (2.19).

As we showed in section 2.1, the solutions to (2.20) converge pointwise to the solutions of the free-space diffusion equation as $h \to 0$. To investigate the regime where h is small but $h \gg a$, we introduce asymptotic expansions in a of the solutions to (2.19) and (2.20) for a small. Our motivation in comparing the asymptotic expansions of the exact solution to (2.19) and the RDME (2.20) derives in part from the asymptotic nature of the solution to the formal continuum limit of (2.20). As mentioned in subsection 2.1, we might expect the solution of the discrete model to approach the solution to

$$\begin{aligned} \frac{\partial p}{\partial t}(\boldsymbol{x},t) &= D\Delta p(\boldsymbol{x},t) - 4\pi Da\delta(\boldsymbol{x})p(\boldsymbol{0},t), \quad \boldsymbol{x} \in \mathbb{R}^3, \\ p(\boldsymbol{x},0) &= \delta(\boldsymbol{x}-\boldsymbol{x}_0), \quad \boldsymbol{x}_0 \neq \boldsymbol{0}, \end{aligned} \tag{2.21}$$

as $h \to 0$. It is true in the distributional sense that the reaction operator

$$-4\pi Da\frac{\delta_{\boldsymbol{j0}}}{h^3} \to -4\pi Da\delta(\boldsymbol{x})$$

as $h \to 0$; however, as we saw in section 2.1, in the continuum limit all reaction effects are lost from the discrete equation (2.20). As described in the introduction, the reaction term in (2.21) may be rigorously treated by defining the entire operator in (2.21) as a member of a one-parameter family of self-adjoint extensions to $\mathbb{R}^3$ of the Laplacian on $\mathbb{R}^3 \setminus \boldsymbol{0}$; see [3, 4, 5]. We denote this family of extensions by the operator $\Delta + \alpha\delta(\boldsymbol{x})$, where α denotes the arbitrary parameter. The solution to (2.21) with the rigorously defined operator $D\Delta - 4\pi Da\delta(\boldsymbol{x})$ [5, Introduction] is the same as the solution to the following pseudopotential model [19, 24]:

$$\begin{aligned} \frac{\partial \rho}{\partial t}(\boldsymbol{x},t) &= D\Delta\rho(\boldsymbol{x},t) - 4\pi Da\delta(\boldsymbol{x})\frac{\partial}{\partial r}\left(r\rho(\boldsymbol{x},t)\right), \quad \boldsymbol{x} \in \mathbb{R}^3, \\ \rho(\boldsymbol{x},0) &= \delta(\boldsymbol{x}-\boldsymbol{x}_0), \quad \boldsymbol{x}_0 \neq \boldsymbol{0}, \end{aligned} \tag{2.22}$$

where $r = |\boldsymbol{x}|$. These delta function and pseudopotential operators were introduced in quantum mechanics to give local potentials whose scattering approximates that of a hard sphere of radius a. The solution to (2.22) is an asymptotic approximation in a of the solution to the SCDLR model (2.19), accurate through terms of order a^2. (See, for example, [27] and compare with the results of subsection 2.2.2.) This suggests that the RDME (2.20) provides an approximation to (2.21) and (2.22), and therefore to the SCDLR model (2.19), even though, as shown in subsection 2.1, it converges to the diffusion equation (i.e., the $\alpha = 0$ case) as the mesh spacing approaches zero.

In section 2.2.1 we derive, through second order, the asymptotic expansion in a of the discrete RDME model (2.20), while in section 2.2.2 we calculate the corresponding expansion of the SCDLR model (2.19). The error between terms of the same order in each of the two expansions is examined in section 2.2.3. In addition, we also examine the relative error between the expansions, truncated after the second order terms, of the solutions to (2.19) and (2.20).

2.2.1. Perturbation theory for the RDME. In order to examine the intermediate situation that h is small but $h \gg a$, we now look at the asymptotics of the solution to (2.20) for a small. We begin by calculating the perturbation expansion of $p_h(\boldsymbol{x},t)$ for a small. Throughout this section we assume that $\boldsymbol{x} = \boldsymbol{x}_{\boldsymbol{j}} = h\boldsymbol{j}$ for some

$\boldsymbol{j} \in \mathbb{Z}^3$, and $\boldsymbol{x}_0 = \boldsymbol{x}_{\boldsymbol{j}_0} = h\boldsymbol{j}_0$ for some $\boldsymbol{j}_0 \in \mathbb{Z}^3$. We also assume that $\boldsymbol{x} \neq \mathbf{0}$ and $\boldsymbol{x}_0 \neq \mathbf{0}$. Using Duhamel's principle, the solution to (2.20) satisfies

$$p_h(\boldsymbol{x},t) = G_h(\boldsymbol{x}-\boldsymbol{x}_0,t) - 4\pi Da \int_0^t G_h(\boldsymbol{x},t-s)p_h(\mathbf{0},s)\,ds. \tag{2.23}$$

We find an asymptotic expansion of p_h in a of the form

$$p_h(\boldsymbol{x},t) = p_h^{(0)}(\boldsymbol{x},t) + a\,p_h^{(1)}(\boldsymbol{x},t) + a^2 p_h^{(2)}(\boldsymbol{x},t) + \cdots,$$

using a Neumann or Born expansion. This expansion is easily obtained by repeatedly replacing $p_h(\mathbf{0},s)$ in (2.23) with the right-hand side of (2.23) evaluated at $\boldsymbol{x} = \mathbf{0}$. Note that this technique leaves an explicit remainder, with which we could perhaps estimate the error between the asymptotic expansion and $p_h(\boldsymbol{x},t)$. For our purposes it suffices to just calculate the first three terms of the expansion. We find

$$\begin{aligned}
p_h(\boldsymbol{x},t) &= G_h(\boldsymbol{x}-\boldsymbol{x}_0,t) - 4\pi Da \int_0^t G_h(\boldsymbol{x},t-s)G_h(\boldsymbol{x}_0,s)\,ds \\
&\qquad + (4\pi Da)^2 \int_0^t G_h(\boldsymbol{x},t-s)\int_0^s G_h(\mathbf{0},s-s')p_h(\mathbf{0},s')\,ds'\,ds \\
&= G_h(\boldsymbol{x}-\boldsymbol{x}_0,t) - 4\pi Da \int_0^t G_h(\boldsymbol{x},t-s)G_h(\boldsymbol{x}_0,s)\,ds \\
&\qquad + (4\pi Da)^2 \int_0^t G_h(\boldsymbol{x},t-s)\int_0^s G_h(\mathbf{0},s-s')G_h(\boldsymbol{x}_0,s')\,ds'\,ds \\
&\qquad + a^3 R_a(\boldsymbol{x},t),
\end{aligned}$$

where $a^3 R_a(\boldsymbol{x},t)$ denotes the remainder when the expansion is stopped at second order. The expansion of (2.20) is then as given in the following.

THEOREM 2.4.

$$p_h^{(0)}(\boldsymbol{x},t) = G_h(\boldsymbol{x}-\boldsymbol{x}_0,t), \tag{2.24}$$

$$p_h^{(1)}(\boldsymbol{x},t) = -4\pi D \int_0^t G_h(\boldsymbol{x},t-s)G_h(\boldsymbol{x}_0,s)\,ds, \tag{2.25}$$

$$p_h^{(2)}(\boldsymbol{x},t) = (4\pi D)^2 \int_0^t G_h(\boldsymbol{x},t-s)\int_0^s G_h(\mathbf{0},s-s')G_h(\boldsymbol{x}_0,s')\,ds'\,ds. \tag{2.26}$$

The formal continuum limit of (2.25) is

$$-4\pi D \int_0^t G(\boldsymbol{x},t-s)G(\boldsymbol{x}_0,s)\,ds. \tag{2.27}$$

Denote this expression by $u(t)$. To find an explicit functional form of $u(t)$ we make use of the Laplace transform. Let $\tilde{f}(s)$ denote the Laplace transform of a function $f(t)$. Taking the transform of (2.27) in t, we find

$$\begin{aligned}
\tilde{u}(s) &= \frac{-1}{4\pi D\,|\boldsymbol{x}|\,|\boldsymbol{x}_0|} e^{-(|\boldsymbol{x}|+|\boldsymbol{x}_0|)\sqrt{s/D}} \\
&= -\frac{|\boldsymbol{x}|+|\boldsymbol{x}_0|}{|\boldsymbol{x}|\,|\boldsymbol{x}_0|}\tilde{G}\big((|\boldsymbol{x}|+|\boldsymbol{x}_0|)\hat{\boldsymbol{x}},s\big),
\end{aligned}$$

where $\hat{\boldsymbol{x}} = \boldsymbol{x}/|\boldsymbol{x}|$ is a unit vector in the direction $\boldsymbol{x}$. Note that $G(|\boldsymbol{x}|\,\hat{\boldsymbol{x}}, t)$ is a radially symmetric function in $\boldsymbol{x}$ and therefore independent of $\hat{\boldsymbol{x}}$. Taking the inverse Laplace transform of $\tilde{u}(s)$, we find

$$-4\pi D \int_0^t G(\boldsymbol{x}, t-s) G(\boldsymbol{x}_0, s)\, ds = -\frac{|\boldsymbol{x}| + |\boldsymbol{x}_0|}{|\boldsymbol{x}|\,|\boldsymbol{x}_0|} G\big((|\boldsymbol{x}| + |\boldsymbol{x}_0|)\hat{\boldsymbol{x}}, t\big). \tag{2.28}$$

2.2.2. Perturbation theory for SCDLR model. There are a number of different techniques that give the asymptotic expansion of solutions to (2.19) as $a \to 0$. We give the exact solution of (2.19) in Theorem 2.5 below and show that it can be directly expanded in a in Theorem 2.6. Alternatively, the first three terms of the expansion can be derived through the use of the pseudopotential approximation (2.22) to the Dirichlet boundary condition in (2.19). The solution to the new diffusion equation with pseudopotential is then itself an asymptotic approximation to the solution of (2.19), accurate through second order in a. This can be seen by comparing the expansion of the exact solution in Theorem 2.6 to the expansion of the pseudopotential solution; see [27].

To derive the exact solution to (2.19), we find it useful to work in spherical coordinates and make the change of variables $\boldsymbol{x} \to (r, \theta, \phi)$, $r \in [a, \infty)$, $\theta \in [0, \pi)$, and $\phi \in [0, 2\pi)$. Similarly, we will let $p(r, \theta, \phi, t) = p(\boldsymbol{x}, t)$ and $\boldsymbol{x}_0 \to (r_0, \theta_0, \phi_0)$.

The exact solution to (2.19) can be found using the Weber transform [23, Chapter "Integral transform"]. Denote by $j_l(r)$ and $\eta_l(r)$ the lth spherical Bessel functions of the first and second kind, respectively, and let

$$q_l(s, u) = j_l(s)\eta_l(u) - \eta_l(s) j_l(u).$$

The forward Weber transform of a function $f(r)$, on the interval $[a, \infty)$, is defined to be

$$F(\lambda, a) = \sqrt{\frac{2}{\pi}} \int_a^\infty q_l(\lambda r, \lambda a) f(r) r^2\, dr.$$

The inverse Weber transform of $F(\lambda, a)$ is then given by

$$f(r) = \sqrt{\frac{2}{\pi}} \int_0^\infty \frac{q_l(\lambda r, \lambda a)}{j_l^2(\lambda a) + \eta_l^2(\lambda a)} F(\lambda, a) \lambda^2\, d\lambda.$$

Using the Weber transform and an expansion in Legendre polynomials, $P_l(\cos(\gamma))$, with $\cos(\gamma) = \cos(\theta)\cos(\theta_0) + \sin(\theta)\sin(\theta_0)\cos(\phi - \phi_0)$, we find the next result.

THEOREM 2.5. *The solution to the free-space diffusion equation with a zero Dirichlet boundary condition on a sphere of radius* a, (2.19), *is given by*

$$p(r, \theta, \phi, t) = \sum_{l=0}^\infty \frac{2l+1}{2\pi^2} \left[\int_0^\infty \frac{q_l(\lambda r, \lambda a)}{j_l^2(\lambda a) + \eta_l^2(\lambda a)} q_l(\lambda r_0, \lambda a) e^{-\lambda^2 D t} \lambda^2\, d\lambda \right] P_l(\cos(\gamma)). \tag{2.29}$$

We again let $\hat{\boldsymbol{x}} = \boldsymbol{x}/|\boldsymbol{x}|$, so that $\hat{\boldsymbol{x}}$ is a unit vector in the same direction as $\boldsymbol{x}$. The first three terms in the expansion of $p(\boldsymbol{x}, t)$ are then given by the following.

THEOREM 2.6. *The solution* (2.29) *to the problem of diffusing to an absorbing sphere* (2.19) *has the asymptotic expansion for small* a,

$$p(\boldsymbol{x}, t) \sim p^{(0)}(\boldsymbol{x}, t) + a p^{(1)}(\boldsymbol{x}, t) + a^2 p^{(2)}(\boldsymbol{x}, t) + \cdots, \tag{2.30}$$

where

$$p^{(0)}(\boldsymbol{x},t) = G(\boldsymbol{x}-\boldsymbol{x}_0,t), \tag{2.31}$$

$$p^{(1)}(\boldsymbol{x},t) = -\frac{|\boldsymbol{x}|+|\boldsymbol{x}_0|}{|\boldsymbol{x}|\,|\boldsymbol{x}_0|}G\big((|\boldsymbol{x}|+|\boldsymbol{x}_0|)\hat{\boldsymbol{x}},t\big), \tag{2.32}$$

$$p^{(2)}(\boldsymbol{x},t) = \frac{2Dt-(|\boldsymbol{x}|+|\boldsymbol{x}_0|)^2}{2Dt\,|\boldsymbol{x}|\,|\boldsymbol{x}_0|}G\big((|\boldsymbol{x}|+|\boldsymbol{x}_0|)\hat{\boldsymbol{x}},t\big). \tag{2.33}$$

Proof. Notice in (2.29) that all a dependence is in the bracketed term. Denoting this term by $R_l(r,r_0,t)$, we can calculate an asymptotic expansion of R_l for small a. This expansion is a straightforward application of the well-known expansions of $j_l(\lambda a)$ [1, equation 10.1.2] and $\eta_l(\lambda a)$ [1, equation 10.1.3] for small a. We find, through second order in a, that

$$R_l(r,r_0,t) \sim R_l^{(0)}(r,r_0,t) + aR_l^{(1)}(r,r_0,t) + a^2R_l^{(2)}(r,r_0,t) + \cdots,$$

where

$$R_l^{(0)}(r,r_0,t) = \int_0^\infty j_l(\lambda r)j_l(\lambda r_0)e^{-\lambda^2Dt}\lambda^2\,d\lambda,$$

$$R_l^{(1)}(r,r_0,t) = \begin{cases} 0, & l>0,\\ \int_0^\infty \left(j_0(\lambda r)\eta_0(\lambda r_0)+\eta_0(\lambda r)j_0(\lambda r_0)\right)e^{-\lambda^2Dt}\lambda^3\,d\lambda, & l=0,\end{cases}$$

$$R_l^{(2)}(r,r_0,t) = \begin{cases} 0, & l>0,\\ \int_0^\infty \left(\eta_0(\lambda r)\eta_0(\lambda r_0)-j_0(\lambda r)j_0(\lambda r_0)\right)e^{-\lambda^2Dt}\lambda^4\,d\lambda, & l=0.\end{cases}$$

Using this expansion, we may derive an expansion for $p(r,\theta,\phi,t)$. We will need several identities involving the spherical Bessel functions. Foremost is the following:

$$\begin{aligned} G(\boldsymbol{x},t) &= \int_{\mathbb{R}^3} e^{-4\pi^2|\boldsymbol{\xi}|^2Dt}e^{2\pi i\boldsymbol{\xi}\cdot\boldsymbol{x}}\,d\boldsymbol{\xi}\\ &= \frac{1}{2\pi^2}\int_0^\infty j_0(\lambda\,|\boldsymbol{x}|)e^{-\lambda^2Dt}\lambda^2\,d\lambda. \end{aligned} \tag{2.34}$$

Here the first integral is the well-known Fourier representation of $G(\boldsymbol{x},t)$. Switching $\boldsymbol{\xi}$ to spherical coordinates in the Fourier integral and performing the angular integrations gives (2.34).

Recall that $j_0(r) = \sin(r)/r$, $\eta_0(r) = -\cos(r)/r$, and $P_0(\cos(\gamma)) = 1$. Substituting these expressions into $R_0^{(1)}(r,r_0,t)$ and $R_0^{(2)}(r,r_0,t)$, evaluating the subsequent integrals, and using (2.34), we obtain (2.32) and (2.33). Using [1, equation 10.1.45] and (2.34), we obtain (2.31). ∎

2.2.3. Error between asymptotic expansions of the SCDLR model and RDME for small h. We now examine the error between corresponding terms of the asymptotic expansions from sections 2.2.1 and 2.2.2. Our main results are as follows.

THEOREM 2.7. *Assume that $\boldsymbol{x} = h\boldsymbol{j} \neq \boldsymbol{0}$, $\boldsymbol{x}_0 = h\boldsymbol{j}_0 \neq \boldsymbol{0}$, and both are fixed as $h \to 0$. Then for all $t > 0$ and h sufficiently small,*

$$\lim_{h\to0} p_h^{(0)}(\boldsymbol{x},t) = p^{(0)}(\boldsymbol{x},t), \quad \textit{with} \quad \left|p_h^{(0)}(\boldsymbol{x},t) - p^{(0)}(\boldsymbol{x},t)\right| = O\left(\frac{h^2}{t^{5/2}}\right), \tag{2.35}$$

$$\lim_{h\to0} p_h^{(1)}(\boldsymbol{x},t) = p^{(1)}(\boldsymbol{x},t), \quad \textit{with} \quad \left|p_h^{(1)}(\boldsymbol{x},t) - p^{(1)}(\boldsymbol{x},t)\right| = O\left(t\,h^{2-\epsilon}\right), \tag{2.36}$$

where ϵ may be chosen arbitrarily small. For all fixed $t > 0$,

$$p_h^{(2)}(\boldsymbol{x}, t) \geq \frac{C}{h}, \quad \textit{for } h \textit{ sufficiently small,} \tag{2.37}$$

where C is strictly positive and constant in h but may depend on t or D.

This theorem demonstrates that the RDME is a convergent asymptotic approximation to the SCDLR model only through first order in the perturbation expansion. For h sufficiently small, the second order term will diverge like $1/h$ as $h \to 0$. The master equation model will then give a good approximation to the SCDLR model only when h is small enough that the first two terms in the asymptotic expansion (2.30) are well approximated, while a is sufficiently small and h sufficiently large that the divergence of higher order terms is small.

Note that the divergence of the second order term follows from the behavior as $h \to 0$ of the time integral of the continuous-time discrete-space Green's function evaluated *at the origin*. The proof of the theorem demonstrates that

$$\int_0^t G_h(\mathbf{0}, s)\, ds = \frac{f_h(t)}{h},$$

where, for t fixed, $f_h(t)$ is bounded from below as $h \to 0$. The nth term in the expansion of $p_h(\boldsymbol{x}, t)$ will involve $n-2$ integrals of $G_h(\mathbf{0}, t)$, so that we expect it to diverge like $1/h^{n-2}$. For example, the $n = 4$ term is given by

$$p_h^{(3)}(\boldsymbol{x}, t) = \int_0^t G_h(\boldsymbol{x}, t-s) \int_0^s G_h(\mathbf{0}, s-s') \int_0^{s'} G_h(\mathbf{0}, s', s'') G_h(\boldsymbol{x}_0, s'')\, ds''\, ds'\, ds,$$

which we would expect to diverge like $1/h^2$. Since the coefficient of the nth term in the expansion is a^{n-1}, we expect the nth term to behave like a^{n-1}/h^{n-2}. For n large this suggests that the heuristic assumption that $h \gg k/4\pi D = a$ from sections 1.1.2 is a reasonable rule of thumb for choosing the mesh size.

Figure 2.3 shows the pointwise error in each of the first three terms of the asymptotic expansion as functions of h, for fixed t, $\boldsymbol{x}$, and $\boldsymbol{x}_0$. Note that for each term the observed numerical convergence (divergence for the second order term) rate agrees with that in Theorem 2.7. Let

$$R_h(\boldsymbol{x}, t, h, a) = p_h^{(0)}(\boldsymbol{x}, t) + a p_h^{(1)}(\boldsymbol{x}, t) + a^2 p_h^{(2)}(\boldsymbol{x}, t)$$

and

$$R(\boldsymbol{x}, t, h, a) = p^{(0)}(\boldsymbol{x}, t) + a p^{(1)}(\boldsymbol{x}, t) + a^2 p^{(2)}(\boldsymbol{x}, t).$$

Figures 2.4 and 2.5 plot the percent relative error between R_h and R,

$$E_{\text{REL}}(\boldsymbol{x}, t, h, a) = 100 \frac{R_h(\boldsymbol{x}, t, h, a) - R(\boldsymbol{x}, t, h, a)}{R(\boldsymbol{x}, t, h, a)}, \tag{2.38}$$

which also represents the percent relative error between the perturbation expansions of $p_h(\boldsymbol{x}, t)$ and $p(\boldsymbol{x}, t)$, the solution to the SCDLR model, truncated after the third term. Notice that for larger values of h the relative error decreases as h decreases, but that as h becomes smaller, the $1/h$ divergence of the second order term begins to dominate and cause E_{REL} to diverge. Both Figures 2.3 and 2.4 are shown for relatively

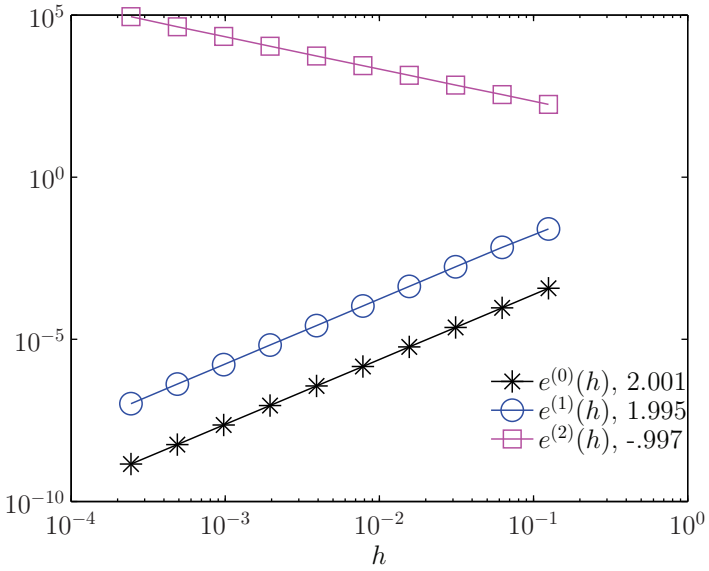

FIG. 2.3. *Absolute error in asymptotic expansion terms.* $e^{(i)}(h) = |p_h^{(i)}(\boldsymbol{x},t) - p^{(i)}(\boldsymbol{x},t)|$, *where* $t = .5$, $\boldsymbol{x} = \boldsymbol{x}_0 = (1/8, 1/8, 1/8)$, *and* $D = 1$. *Numbers in the inset within the figure denote the slope of the best fit line through each curve.*

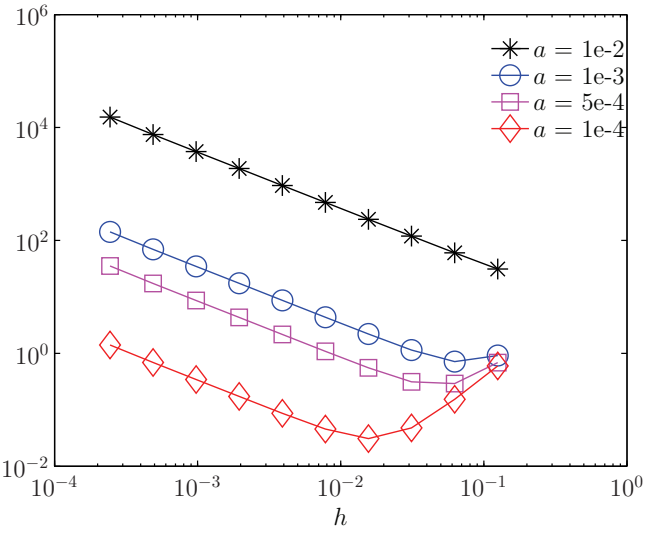

FIG. 2.4. *Percent relative error in perturbation expansions through second order. Each curve plots* $E_{REL}(\boldsymbol{x},t,h,a)$ *versus* h *for different values of the reaction radius,* a. *For all curves* $t = .5$, $\boldsymbol{x} = \boldsymbol{x}_0 = (1/8, 1/8, 1/8)$, *and* $D = 1$.

large t values. Figure 2.5 shows the behavior of E_{REL} at a shorter time, when both $p_h(\boldsymbol{x},t)$ and $p(\boldsymbol{x},t)$ have relaxed less. The details of the numerical methods used in calculating the terms of the asymptotic expansions are explained in Appendix C.

For $a \leq 10^{-3}$ the overall relative error can be reduced below one percent. In physical units, appropriate for considering chemical systems at the scale of a eukaryotic

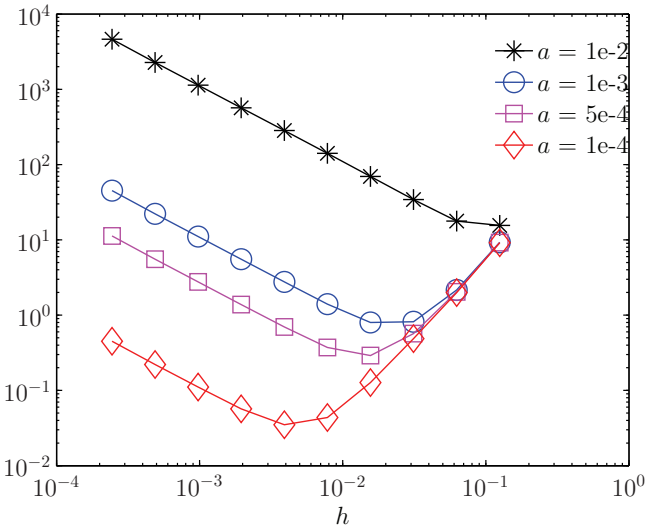

FIG. 2.5. *Percent relative error in perturbation expansions through second order. Each curve plots* $E_{REL}(\boldsymbol{x}, t, h, a)$ *versus* h *for different values of the reaction radius,* a*. For all curves* $t = .038147$*,* $\boldsymbol{x} = \boldsymbol{x}_0 = (1/8, 1/8, 1/8)$*, and* $D = 1$*.*

cell, D would have units of square micrometers per second, t units of seconds, and $\boldsymbol{x}$, $\boldsymbol{x}_0$, and a units of micrometers. This *suggests* that for physical reaction-radii of one nanometer or less the RDME may be a good approximation to a diffusion limited reaction. While physical reaction-radii have not been experimentally determined for most biological reactions, it has been found experimentally that the LexA DNA binding protein has a physical binding potential of width ~ 5 Å [30]. We caution, however, that these results are valid only for the truncated perturbation expansions and do not necessarily hold for the error between the exact solutions $p_h(\boldsymbol{x}, t)$ and $p(\boldsymbol{x}, t)$. Moreover, for realistic biophysical systems, one would frequently be interested in volumes where more than one of each substrate is present, a case we have not examined herein.

Proof of Theorem 2.7. The validity of (2.35) has already been established in Theorem B.1. Lemma 2.2 and Corollary B.2 imply that for all h and ϵ sufficiently small, and all $t \geq 0$,

$$\sup_{t\in[0,\infty)} |G_h(\boldsymbol{x}, t-s)G_h(\boldsymbol{x}_0, s) - G(\boldsymbol{x}, t-s)G(\boldsymbol{x}_0, s)| \leq Ch^{2-\epsilon},$$

with C independent of t, s, and h. Recalling (2.28), (2.32), and (2.25), we find

$$\left| p_h^{(1)}(\boldsymbol{x}, t) - p^{(1)}(\boldsymbol{x}, t) \right| \leq C\, t\, h^{2-\epsilon},$$

which proves (2.36). We now consider the divergence of $p_h^{(2)}(\boldsymbol{x}, t)$. The nonnegativity of $G_h(\boldsymbol{x}, t)$ for all $\boldsymbol{x}$ and $t \geq 0$ implies that for all $t > 3\delta > 0$,

$$p_h^{(2)}(\boldsymbol{x}, t) \geq (4\pi D)^2 \int_{2\delta}^{t-\delta} G_h(\boldsymbol{x}, t-s) \int_{s-\delta}^{s} G_h(\boldsymbol{0}, s-s')G_h(\boldsymbol{x}_0, s')\, ds'\, ds.$$

We subsequently denote by C a generic positive constant independent of h but dependent on t. Note that $G(\boldsymbol{x}, t)$ is positive for all $\boldsymbol{x}$ and all $t > 0$. Uniform convergence

in time of $G_h(\boldsymbol{x},t)$ to $G(\boldsymbol{x},t)$ (Theorem B.1) implies that ϵ and h may be taken sufficiently small so that

$$\begin{aligned}\inf_{s\in(2\delta,t-\delta)} G_h(\boldsymbol{x},t-s) &\geq \inf_{s\in(2\delta,t-\delta)} G(\boldsymbol{x},t-s) - \epsilon \\ &\geq C > 0,\end{aligned}$$

and similarly

$$\inf_{s'\in(\delta,t-\delta)} G_h(\boldsymbol{x}_0,s') \geq C > 0.$$

We then find that, for all h sufficiently small,

$$\begin{aligned}p_h^{(2)}(\boldsymbol{x},t) &\geq C\int_{2\delta}^{t-\delta}\int_{s-\delta}^{s} G_h(\mathbf{0},s-s')\,ds'\,ds \\ &\geq C\int_0^{\delta} G_h(\mathbf{0},s)\,ds. \qquad (2.39)\end{aligned}$$

$G_h(\mathbf{0},s)$ has the Fourier representation

$$G_h(\mathbf{0},s) = \frac{1}{h^3}\iiint_{\left[\frac{-1}{2}\cdots\frac{1}{2}\right]^3} e^{-4Ds\sum_{k=1}^3 \sin^2(\pi y_k)/h^2}\,d\boldsymbol{y}.$$

As the integrand in the above integral is nonnegative, we may apply Fubini's theorem to switch the order of integration in (2.39). We find

$$p_h^{(2)}(\boldsymbol{x},t) \geq \frac{C}{h}\iiint_{\left[\frac{-1}{2}\cdots\frac{1}{2}\right]^3} \frac{1}{\sum_{k=1}^3 \sin^2(\pi y_k)}\left(1-e^{-4D\delta\sum_{k=1}^3 \sin^2(\pi y_k)/h^2}\right)\,d\boldsymbol{y}.$$

Switching to spherical coordinates in the integral, we have that

$$\begin{aligned}p_h^{(2)}(\boldsymbol{x},t) &\geq \frac{C}{h}\int_0^{1/2}\left(1-e^{-16D\delta r^2/h^2}\right)\,dr \\ &= \frac{C}{h}\left(\frac{1}{2}-\sqrt{\frac{\pi}{t}}\frac{h}{8}\operatorname{erf}\left(\frac{2\sqrt{t}}{h}\right)\right). \qquad (2.40)\end{aligned}$$

Here we have used that $\pi y \geq \sin(\pi y) \geq 2y$ on $[0,1/2]$. The last term in parenthesis in (2.40) approaches zero as $h\to 0$, and therefore

$$p_h^{(2)}(\boldsymbol{x},t) \geq \frac{C}{h}$$

for h sufficiently small, with C strictly positive. ∎

3. Conclusions. We have shown that as the mesh spacing approaches zero in the RDME model, particles undergoing a bimolecular reaction never react but simply diffuse. In contrast, the relative errors of the truncated asymptotic expansions shown in Figures 2.4 and 2.5 suggest that for physically reasonable parameters values the mesh spacing in the RDME may be chosen to give a good approximation of an SCDLR model. Notice in Figure 2.5 that the mesh spacing for the minimal relative error is generally more than a factor of ten larger than the reaction-radius. This suggests that choosing the mesh spacing to satisfy the physically derived lower bound, (1.6),

may be a good rule of thumb. Note, however, that good agreement between the truncated asymptotic expansions does not necessarily guarantee good agreement of the actual solutions of the two models. We hope to report on the error between the solutions to the RDME and the SCDLR models, for biologically relevant parameter values, in future work. Toward that end, we would like to examine this error in a more biologically relevant (bounded) domain. (The restriction to $\mathbb{R}^3$ in the current work was made to simplify the mathematical analysis, and may increase the error between the two models due to effects at infinity.)

The results of section 2.2.3 suggest a means by which to improve the accuracy of the RDME as an approximation to a diffusion limited reaction: modifying/renormalizing the bimolecular reaction rate, k/h^3, so that the second order term in the asymptotic expansion of the solution to the RDME converges to the corresponding term in the asymptotic expansion of the SCDLR model. Note that this may require changing the discrete bimolecular reaction operator to couple neighboring voxels, and would presumably correspond to modifying it to converge to a pseudopotential reaction operator like that in (2.22).

Finally, we would like to point out that it should be an easy modification to extend the results of this work to $\mathbb{R}^d$ for all $d \geq 2$. In particular, it appears that the second order term in the asymptotic expansion of the RDME diverges like $\log(h)$ in two dimensions, and $1/h^{d-2}$ in d dimensions with $d > 2$. In one dimension the solution of the continuum model, (2.21), is well defined, and we expect the solution to the RDME to converge to it.

Appendix A. Properties of the solution, $p_h(\boldsymbol{x_j}, t)$, to (2.6). In this appendix we prove several properties of the solution, $p_h(\boldsymbol{x_j}, t)$, to (2.6). In particular, we show that $p_h(\boldsymbol{x_j}, t)$ is positive for $t > 0$, continuous, and that the binding time distribution, $F_h(t)$, is a rigorous (possibly defective) probability distribution.

We begin by defining some basic notation that we will use in discussing the action of the solution operator to (2.6) on lattice functions. Denote by $\mathbb{Z}^3 h$ the set of points $\{\boldsymbol{x_i} = h\boldsymbol{i} \mid \boldsymbol{i} \in Z^3\}$. The notation a or $a(\cdot)$ will subsequently be used to denote a lattice function, with the notation $a(\boldsymbol{x_i})$ indicating the value of that function at the lattice point $\boldsymbol{x_i}$. We define $l_1(\mathbb{Z}^3 h)$ to represent the space of lattice functions a such that the norm

$$\|a\|_1 = \sum_{\boldsymbol{i} \in \mathbb{Z}^3} |a(\boldsymbol{x_i})| \, h^3 < \infty,$$

and similarly, $l_2(\mathbb{Z}^3 h)$ is the set of lattice functions a such that the norm

$$\|a\|_2 = \left(\sum_{\boldsymbol{i} \in \mathbb{Z}^3} |a(\boldsymbol{x_i})|^2 \, h^3 \right)^{\frac{1}{2}} < \infty.$$

Letting a and b be elements of $l_2(\mathbb{Z}^3 h)$, we denote the $l_2(\mathbb{Z}^3 h)$ inner product by

$$\langle a, b \rangle = \sum_{\boldsymbol{i} \in \mathbb{Z}^3} a(\boldsymbol{x_i}) \, b(\boldsymbol{x_i}) \, h^3.$$

Define

$$\delta_h(\boldsymbol{x_i}, \boldsymbol{x_j}) = \frac{1}{h^3} \delta_{\boldsymbol{ij}},$$

with $\delta_h(\cdot, \boldsymbol{x_j})$ denoting the lattice function that is zero everywhere except at $\boldsymbol{x_j}$, where it has the value $1/h^3$. We let L represent the operator on the right-hand side of (2.6), with action on a lattice function a defined by

$$La = D\Delta_h a - k \langle \delta_h(\cdot, \mathbf{0}), a \rangle \, \delta_h(\cdot, \mathbf{0}) \, .$$

The boundedness of the operators Δ_h and $\langle \delta_h(\cdot, \mathbf{0}), \cdot \rangle \, \delta_h(\cdot, \mathbf{0})$ on $l_1(\mathbb{Z}^3 h)$ and $l_2(\mathbb{Z}^3 h)$ imply that L is also a bounded operator on both these spaces. The group

$$e^{Lt}, \quad t \in \mathbb{R},$$

is therefore a bounded operator in both spaces, analytic (in the operator norm sense) for all $t \in \mathbb{R}$. Denote by $p_h(t)$ the lattice function on $\mathbb{Z}^3 h$ with values given by the solution, $p_h(\boldsymbol{x_j}, t)$, to (2.6). $p_h(t)$ may be written as

$$p_h(t) = e^{Lt} \delta_h(\cdot, \boldsymbol{x}_{\boldsymbol{j}_0}),$$

with

$$p_h(\boldsymbol{x_j}, t) = \left(e^{Lt} \delta_h(\cdot, \boldsymbol{x}_{\boldsymbol{j}_0})\right)(\boldsymbol{x_j}) = \left\langle e^{Lt} \delta_h(\cdot, \boldsymbol{x}_{\boldsymbol{j}_0}), \delta_h(\cdot, \boldsymbol{x_j}) \right\rangle . \tag{A.1}$$

The norm analyticity of $\exp(Lt)$ for all $t \in \mathbb{R}$ then implies that, for each fixed $\boldsymbol{x_j}$, $p_h(\boldsymbol{x_j}, t)$ is continuous in t (since the inner product (A.1) will vary continuously in t). Analyticity of $p_h(\boldsymbol{x_j}, t)$ in t will follow in a similar manner.

The action of the operator $\exp\left(-k \langle \delta_h(\cdot, \mathbf{0}), \cdot \rangle \, \delta_h(\cdot, \mathbf{0}) \, t\right)$ may be explicitly calculated for any lattice function a in $l_1(\mathbb{Z}^3 h)$ or $l_2(\mathbb{Z}^3 h)$. From the Taylor series definition of the operator we have

$$\begin{aligned} e^{-k\langle \delta_h(\cdot,\mathbf{0}), \cdot \rangle \delta_h(\cdot,\mathbf{0}) \, t} a &= \sum_{n=0}^{\infty} \frac{(-kt)^n}{n!} \left(\langle \delta_h(\cdot, \mathbf{0}), \cdot \rangle \, \delta_h(\cdot, \mathbf{0}) \right)^n a \\ &= a + a_{\mathbf{0}} \left(\sum_{n=1}^{\infty} \frac{(-kt)^n}{n! \, h^{3n}} \right) \delta_h(\cdot, \mathbf{0}) h^3 \\ &= a - a_{\mathbf{0}} \, \delta_h(\cdot, \mathbf{0}) h^3 + a_{\mathbf{0}} \, e^{-kt/h^3} \delta_h(\cdot, \mathbf{0}) h^3, \end{aligned}$$

which implies that $\exp\left(-k \langle \delta_h(\cdot, \mathbf{0}), \cdot \rangle \, \delta_h(\cdot, \mathbf{0}) \, t\right)$ maps nonnegative lattice functions, with the exception of the zero function, to positive lattice functions for all $t > 0$. The evolution operator for the discrete-space continuous-time diffusion equation, $\exp D\Delta_h t$, will also map nonnegative, nonzero lattice functions to positive lattice functions for $t > 0$. The Lie–Trotter product formula for self-adjoint bounded operators implies that

$$e^{Lt} = \lim_{n \to \infty} \left(e^{D\Delta_h t/n} e^{-k\langle \delta_h(\cdot,\mathbf{0}), \cdot \rangle \delta_h(\cdot,\mathbf{0}) \, t/n} \right)^n ,$$

where the limit is taken in the $l_2(\mathbb{Z}^3 h)$ induced operator norm. Using this relation in (A.1), we may then conclude that $p_h(\boldsymbol{x_j}, t)$ is positive for positive times.

Denote by $G_h(\cdot - \boldsymbol{x}_{\boldsymbol{j}_0}, t)$ the lattice function with values $G_h(\boldsymbol{x_i} - \boldsymbol{x}_{\boldsymbol{j}_0}, t)$ (and likewise by $G_h(\cdot, t)$ the lattice function with values $G_h(\boldsymbol{x_i}, t)$). Starting with (2.11), using the positivity of $p_h(\boldsymbol{x_j}, t)$ and $G_h(\boldsymbol{x_j}, t)$ for $t > 0$, and then taking the $l_1(\mathbb{Z}^3 h)$ norm, we find

$$\|p_h(t)\|_1 < \|G_h(\cdot - \boldsymbol{x}_{\boldsymbol{j}_0}, t)\|_1 = 1 \quad \forall t > 0.$$

(Here we have used that $\|G_h(\cdot,t)\|_1 = 1$.)

We conclude by showing that the probability distribution needed for the molecules to have reacted,

$$F_h(t) = k\int_0^t p_h(\mathbf{0},s)\,ds,$$

is a rigorously defined (possibly defective) probability distribution (in the sense of the definition of [18]). It is immediately apparent from the preceding properties of $p_h(\boldsymbol{x_j},t)$ that $F_h(t)$ is nonnegative, continuous for $t>0$, right-continuous at $t=0$, and monotone nondecreasing. By definition, $F_h(0)=0$. The only remaining condition to show is that $F_h(\infty)\le 1$, i.e., that $F_h(t)$ is a (possibly defective) distribution. Rearranging (2.11), we have that

$$p_h(\boldsymbol{x_j},t) + k\int_0^t G_h(\boldsymbol{x_j},t-s)\,p_h(\mathbf{0},s)\,ds = G_h(\boldsymbol{x_j}-\boldsymbol{x_{j_0}},t).$$

Notice that each term above is positive for $t>0$. Multiplying by h^3 and taking the sum over all $\boldsymbol{j}\in\mathbb{Z}^3$ on each side, we find

$$\|p_h(t)\|_1 + k\int_0^t \|G_h(\cdot,t-s)\|_1\,p_h(\mathbf{0},s)\,ds = \|G_h(\cdot-\boldsymbol{x_{j_0}},t)\|_1.$$

Here we have used Fubini's theorem to exchange the sum and integral in the second term on the left-hand side. As $\|G_h(\cdot,t)\|_1=1$, we conclude that

$$\|p_h(t)\|_1 + F_h(t) = 1,$$

so that $F_h(t) = 1-\|p_h(t)\|_1 < 1$. We therefore conclude that $F_h(\infty)\le 1$ so that $F_h(t)$ is a (possibly defective) probability distribution.

Appendix B. Convergence of the Green's function for the discrete-space continuous-time diffusion equation. We prove the following convergence theorem.

THEOREM B.1. *Let $\boldsymbol{x_j} = h\boldsymbol{j}$ remain fixed as $h\to 0$. Then for all $\boldsymbol{x_j}$, all $t\ge\delta>0$ with δ fixed, and $h>0$ sufficiently small,*

$$|G_h(\boldsymbol{x_j},t) - G(\boldsymbol{x_j},t)| \le C\frac{h^2}{\delta^{5/2}}. \tag{B.1}$$

Here C is independent of t, h, and $\boldsymbol{x_j}$.

In addition, for $\boldsymbol{x_j}$ fixed as $h\to 0$ and $\boldsymbol{x_j}\neq\mathbf{0}$, $G_h(\boldsymbol{x_j},t)\to G(\boldsymbol{x_j},t)$ uniformly in all $t\ge 0$ as $h\to 0$.

Proof. We begin by proving (B.1). G_h has the representation

$$G_h(\boldsymbol{x_j},t) = \iiint_{\left[\frac{-1}{2h}\cdots\frac{1}{2h}\right]^3} e^{-4Dt\sum_{k=1}^3 \frac{\sin^2(\pi h\boldsymbol{\xi}_k)}{h^2}} e^{2\pi i(\boldsymbol{x_j},\boldsymbol{\xi})}\,d\boldsymbol{\xi}.$$

Similarly,

$$G(\boldsymbol{x_j},t) = \iiint_{\mathbb{R}^3} e^{-4Dt\pi^2|\boldsymbol{\xi}|^2} e^{2\pi i(\boldsymbol{x_j},\boldsymbol{\xi})}\,d\boldsymbol{\xi}.$$

We find

(B.2)
$$|G_h(\boldsymbol{x_j},t)-G(\boldsymbol{x_j},t)| \leq \iiint_{\left[\frac{-1}{2h}\cdots\frac{1}{2h}\right]^3} \left| e^{-4Dt\sum_{k=1}^3 \frac{\sin^2(\pi h\boldsymbol{\xi}_k)}{h^2}} - e^{-4Dt\pi^2|\boldsymbol{\xi}|^2}\right| d\boldsymbol{\xi} + \iiint_{R^3-\left[\frac{-1}{2h}\cdots\frac{1}{2h}\right]^3} e^{-4Dt\pi^2|\boldsymbol{\xi}|^2}\, d\boldsymbol{\xi}.$$

Denote these last two integrals by I and II, respectively. The second integral may be bounded by expanding the domain of integration to the exterior of the sphere of radius $1/2h$. Switching to polar coordinates, this gives

$$\begin{aligned} II &\leq 4\pi \int_{\frac{1}{2h}}^{\infty} r^2 e^{-4Dt\pi^2 r^2}\, dr \\ &= \frac{1}{4\pi Dth} e^{-\pi^2 Dt/h^2} + \frac{1}{8(\pi Dt)^{3/2}} \operatorname{erfc}\left(\frac{\pi\sqrt{Dt}}{h}\right). \end{aligned}$$

Using that (see [1, equation 7.1.13])

$$\operatorname{erfc}(r) \leq e^{-r^2}, \quad r \geq 0, \tag{B.3}$$

we find

$$II \leq \frac{1}{h(4\pi Dt)^{3/2}} \left(2\sqrt{\pi Dt}+h\right) e^{-\pi^2 Dt/h^2} \quad \forall t>0. \tag{B.4}$$

For h sufficiently small this error bound will satisfy (B.1).

To bound I, we begin by Taylor expanding the first term of the integrand in I about the point $\pi h\boldsymbol{\xi}$. Note that $\pi h\boldsymbol{\xi} \in [-\pi/2,\pi/2]^3$ even as h changes. Let $\boldsymbol{y}=\pi h\boldsymbol{\xi}$, and define

$$f(\boldsymbol{y}) = 4Dt\sum_{k=1}^3 \frac{\sin^2(y_k)\pi^2\boldsymbol{\xi}_k^2}{y_k^2}.$$

$e^{-f(\boldsymbol{y})}$ has the two-term Taylor expansion with remainder

$$e^{-f(\boldsymbol{y})} = e^{-4Dt\pi^2|\boldsymbol{\xi}|^2} + \frac{1}{2}\left(\boldsymbol{y}, D^2 e^{-f(\bar{\boldsymbol{y}})}\boldsymbol{y}\right), \quad \bar{\boldsymbol{y}} \in \left[-\frac{1}{2},\frac{1}{2}\right]^3.$$

Here D^2 denotes the matrix of second derivatives of $f(\boldsymbol{y})$, and the first derivative term disappears since the gradient of $f(\boldsymbol{y})$ is zero at $\boldsymbol{y}=\boldsymbol{0}$. The second derivative term is given by

$$\left(D^2 e^{-f(\boldsymbol{y})}\right)_{i,j} = -\left(\frac{\partial^2 f}{\partial y_i \partial y_j}(\boldsymbol{y}) - \frac{\partial f}{\partial y_i}(\boldsymbol{y})\frac{\partial f}{\partial y_j}(\boldsymbol{y})\right) e^{-f(\boldsymbol{y})},$$

where

$$\frac{\partial f}{\partial y_i}(\boldsymbol{y}) = -4Dt\pi^2\xi_i^2\left(\frac{2\sin^2(y_i)}{y_i^3} - \frac{\sin(2y_i)}{y_i^2}\right)$$

and

$$\frac{\partial^2 f}{\partial y_i \partial y_j}(\boldsymbol{y}) = \begin{cases} 0, & i \neq j, \\ 4Dt\pi^2\xi_i^2 \left(2y_i^2\cos(2y_i) - 4y_i\sin(2y_i) + 6\sin^2(y_i)\right)/y_i^4. \end{cases}$$

Since $|\bar{y}_i| \leq 1/2$, we may uniformly bound in $\boldsymbol{y}$ the remainders for the one-term Taylor expansions of the derivatives of $f(\bar{\boldsymbol{y}})$. We find

$$D^2 e^{-f(\bar{\boldsymbol{y}})} \leq e^{-f(\bar{\boldsymbol{y}})} A(\boldsymbol{\xi}, t),$$

where

$$A_{i,j}(\boldsymbol{\xi}, t) = \begin{cases} O(t^2\xi_i^2\xi_j^2), & i \neq j, \\ O(t^2\xi_i^4 + t\xi_i^2), & i = j. \end{cases}$$

Letting $\|\cdot\|_2$ denote the matrix norm induced by the Euclidean vector norm, this estimate gives the bound

$$\begin{aligned} \left(\boldsymbol{y}, D^2 e^{-f(\bar{\boldsymbol{y}})}\boldsymbol{y}\right) &\leq e^{-f(\bar{\boldsymbol{y}})} \|A(\boldsymbol{\xi}, t)\|_2 \left|\boldsymbol{y}\right|^2 \\ &\leq C e^{-f(\bar{\boldsymbol{y}})} \|A(\boldsymbol{\xi}, t)\|_F \left|\boldsymbol{\xi}\right|^2 h^2, \end{aligned} \tag{B.5}$$

where $\|\cdot\|_F$ denotes the matrix Frobenius norm. Letting $M_n(\boldsymbol{\xi})$ be a three-dimensional monomial of degree n, we have

$$\begin{aligned} \|A(\boldsymbol{\xi}, t)\|_F &= \left(O(t^4 M_8(\boldsymbol{\xi})) + O(t^2 M_4(\boldsymbol{\xi}))\right)^{\frac{1}{2}} \\ &\leq O(t^2 \left|\boldsymbol{\xi}\right|^4) + O(t \left|\boldsymbol{\xi}\right|^2), \end{aligned} \tag{B.6}$$

for specific monomials $M_8(\boldsymbol{\xi})$ and $M_4(\boldsymbol{\xi})$. (This follows since $M_{2n}(\boldsymbol{\xi}) \leq C \left|\boldsymbol{\xi}\right|^{2n}$ for all n.) Moreover, since

$$\sin^2(x) \geq \frac{4}{\pi^2} x^2 \quad \forall x \in \left[-\frac{\pi}{2}, \frac{\pi}{2}\right],$$

we have that

$$e^{-f(\bar{\boldsymbol{y}})} \leq e^{-16Dt|\boldsymbol{\xi}|^2}. \tag{B.7}$$

Combining the two preceding estimates, (B.6) and (B.7), with (B.5), we find

$$\left(\boldsymbol{y}, D^2 e^{-f(\bar{\boldsymbol{y}})}\boldsymbol{y}\right) \leq \left(O(t^2 \left|\boldsymbol{\xi}\right|^6) + O(t \left|\boldsymbol{\xi}\right|^4)\right) e^{-16Dt|\boldsymbol{\xi}|^2} h^2.$$

This estimate implies that

$$\begin{aligned} I &\leq h^2 \iiint_{\left[\frac{-1}{2h} \cdots \frac{1}{2h}\right]^3} \left(O(t^2 \left|\boldsymbol{\xi}\right|^6) + O(t \left|\boldsymbol{\xi}\right|^4)\right) e^{-16Dt|\boldsymbol{\xi}|^2} \, d\boldsymbol{\xi} \\ &\leq h^2 \int_0^\infty \left(O(t^2 r^8) + O(t\, r^6)\right) e^{-16Dtr^2} \, dr, \\ &= O\left(\frac{h^2}{t^{5/2}}\right). \end{aligned} \tag{B.8}$$

For $t \geq \delta$ the desired bound in (B.1) follows.

We now prove the second assertion of the theorem, that for $\boldsymbol{x_j} \neq \mathbf{0}$ and fixed as $h \to 0$, $G_h(\boldsymbol{x_j}, t) \to G(\boldsymbol{x_j}, t)$ as $h \to 0$ uniformly in all $t \geq 0$. To prove the assertion, we find it necessary to treat separately very short and all other times. Let $a_h = h^{-1-\mu}$ with $\mu \in (0,1)$, so that $a_h h^2 \to 0$ and $a_h h \to \infty$ as $h \to 0$. The condition $a_h h \to \infty$ as $h \to 0$ will turn out to be necessary to prove uniform convergence for short times. We wish to show that

$$\lim_{h \to 0} \sup_{t \in [0,\infty)} |G_h(\boldsymbol{x_j}, t) - G(\boldsymbol{x_j}, t)| = 0.$$

This is equivalent to proving that for any $\epsilon > 0$ and all h sufficiently small

$$\sup_{t \in [0, a_h h^2)} |G_h(\boldsymbol{x_j}, t) - G(\boldsymbol{x_j}, t)| < \epsilon \tag{B.9}$$

and

$$\sup_{t \in [a_h h^2, \infty)} |G_h(\boldsymbol{x_j}, t) - G(\boldsymbol{x_j}, t)| < \epsilon. \tag{B.10}$$

We begin by proving (B.10). Equation (B.2) bounds the error for fixed t by two terms, I and II, with II satisfying equation (B.4). Let $0 < R < 1/(2h)$. I satisfies

$$\begin{aligned} I \leq & \iiint_{|\boldsymbol{\xi}|<R} \left| e^{-4Dt \sum_{k=1}^3 \frac{\sin^2(\pi h \boldsymbol{\xi}_k)}{h^2}} - e^{-4Dt\pi^2 |\boldsymbol{\xi}|^2} \right| d\boldsymbol{\xi} \\ & + \iiint_{\left[\frac{-1}{2h} \cdots \frac{1}{2h}\right]^3 - \{|\boldsymbol{\xi}|<R\}} \left| e^{-4Dt \sum_{k=1}^3 \frac{\sin^2(\pi h \boldsymbol{\xi}_k)}{h^2}} - e^{-4Dt\pi^2 |\boldsymbol{\xi}|^2} \right| d\boldsymbol{\xi}. \end{aligned}$$

We subsequently label the two terms on the right-hand side by I_a and I_b, respectively. In what follows, C will denote an arbitrary constant, independent of h and t. The argument giving (B.8) holds for I_a and shows that

$$\begin{aligned} I_a &\leq Ch^2 \iiint_{|\boldsymbol{\xi}|<R} \left(t^2 |\boldsymbol{\xi}|^6 + t |\boldsymbol{\xi}|^4 \right) e^{-16Dt|\boldsymbol{\xi}|^2} d\boldsymbol{\xi} \\ &\leq Ch^2 R^3 \iiint_{|\boldsymbol{\xi}|<R} \left(t^2 |\boldsymbol{\xi}|^3 + t |\boldsymbol{\xi}| \right) e^{-16Dt|\boldsymbol{\xi}|^2} d\boldsymbol{\xi} \\ &= C \frac{h^2 R^3}{t} \quad \forall t > 0. \end{aligned} \tag{B.11}$$

Using (B.7), we have that

$$\begin{aligned} I_b &\leq C \int_R^\infty r^2 e^{-16Dtr^2} dr \\ &= \frac{C}{t^{3/2}} \left[8R\sqrt{t} e^{-16DtR^2} + \sqrt{\pi} \operatorname{erfc}\left(4R\sqrt{Dt} \right) \right], \end{aligned}$$

which by (B.3) implies

$$I_b \leq \frac{C}{t^{3/2}} \left[8R\sqrt{t} + \sqrt{\pi} \right] e^{-16DtR^2} \quad \forall t > 0. \tag{B.12}$$

To summarize, we have shown that

$$|G_h(\boldsymbol{x_j}, t) - G(\boldsymbol{x_j}, t)| \leq I_a + I_b + II,$$

where

$$\begin{aligned} I_a &\leq C\frac{h^2R^3}{t}, \\ I_b &\leq \frac{C}{t^{3/2}}\left[8R\sqrt{t}+\sqrt{\pi}\right]e^{-16DtR^2}, \\ II &\leq \frac{1}{h(8\pi Dt)^{3/2}}\left(2\sqrt{\pi Dt}+h\right)e^{-\pi^2Dt/h^2}. \end{aligned} \tag{B.13}$$

We now show that this error can be made uniformly small in t for $t \geq a_h h^2$. Substituting this inequality into (B.13), we find

$$\begin{aligned} I_a &\leq C\frac{R^3}{a_h}, \\ I_b &\leq \frac{C}{(a_h h^2)^{3/2}}\left[8R\sqrt{a_h}h+\sqrt{\pi}\right]e^{-16Da_hh^2R^2}, \\ II &\leq \frac{1}{(8\pi Da_hh^2)^{3/2}}\left(2\sqrt{\pi Da_h}+1\right)e^{-\pi^2Da_h}. \end{aligned} \tag{B.14}$$

Clearly II will be arbitrarily small for all h sufficiently small, so it remains to show that R and a_h can be chosen such that I_a and I_b approach zero as $h \to 0$. This will hold if

$$\begin{aligned} \lim_{h\to 0}\frac{R^3}{a_h} &= 0, \\ \lim_{h\to 0} a_h h^2 R^2 &= \infty, \end{aligned} \tag{B.15}$$

with $0 < R < 1/(2h)$, $a_h h \to \infty$ as $h \to 0$, and $a_h h^2 \to 0$ as $h \to 0$. As mentioned earlier, we let $a_h = h^{-1-\mu}$ with $\mu \in (0,1)$. In addition, let $R = h^{-\alpha}/2$ with $\alpha \in (0,1)$. Note that this choice of α allows $0 < R < 1/(2h)$ for h small, as required. Equation (B.15) then holds if

$$\begin{aligned} 1+\mu-3\alpha &> 0, \\ 2\alpha+\mu-1 &> 0. \end{aligned} \tag{B.16}$$

These equations have an infinite number of valid solutions which also satisfy the other necessary conditions on R and a_h. For example, $\alpha = 1/4$ and $\mu = 3/4$. We have therefore shown that (B.10) holds.

We now prove that (B.9) holds. We denote the first nonzero component of $\boldsymbol{x_j}$ by x. Note that $G_h(\boldsymbol{x_j}, t)$ may be written in terms of the solution to the one-dimensional continuous-time discrete-space diffusion equation, $g_h(x_{j_k}, t)$, as

$$G_h(\boldsymbol{x_j}, t) = \prod_{k=1}^{3} g_h(x_{j_k}, t).$$

Nonnegativity of $g_h(x_{j_k}, t)$ and the conservation relation

$$\sum_{n=-\infty}^{\infty} g_h(nh, t)h = 1$$

imply

$$G_h(\boldsymbol{x_j}, t) \leq \frac{1}{h^2} g_h(x, t).$$

Without loss of generality, we now assume that $x > 0$. Then for any positive number, λ,

$$\frac{1}{h^2} g_h(x, t) \leq \frac{1}{h^2} \sum_{n=-\infty}^{\infty} e^{\lambda n - \lambda x/h} g_h(nh, t).$$

We define

$$M(\lambda, t) = \sum_{n=-\infty}^{\infty} e^{\lambda n} g_h(nh, t).$$

Note that $g_h(nh, t)h$ is the probability distribution for a continuous-time random walk in $\mathbb{R}^1$ with nearest-neighbor transition rate D/h^2 and lattice spacing h. Likewise, $M(\lambda, t)h$ is the moment generating function associated with $g_h(nh, t)h$. Differentiating $M(\lambda, t)$ and using that $g_h(nh, t)$ satisfies the continuous-time discrete-space diffusion equation, we find

$$\frac{dM}{dt}(\lambda, t) = \frac{2D}{h^2} \left(\cosh(\lambda) - 1\right) M(\lambda, t).$$

As $g_h(nh, 0) = \delta_{n0}/h$, we have $M(\lambda, 0) = 1/h$. This implies

$$\begin{aligned} M(\lambda, t) &= \frac{1}{h} e^{(\cosh(\lambda)-1)(2Dt/h^2)} \\ &\leq \frac{1}{h} e^{(\cosh(\lambda)-1)(2Da_h)}, \end{aligned}$$

so that

$$\frac{1}{h^2} g_h(x, t) \leq \frac{1}{h^3} e^{-\lambda x/h} e^{(\cosh(\lambda)-1)(2Da_h)}.$$

Since λ is arbitrary, we now assume that λ is small. We may then expand the $\cosh(\lambda)$ term so that

$$\frac{1}{h^2} g_h(x, t) \leq \frac{1}{h^3} e^{-\lambda x/h} e^{Da_h\lambda^2} e^{O(\lambda^4 a_h)}.$$

Choosing $\lambda = x/2Da_hh$, which will be small for h sufficiently small, we find

$$\frac{1}{h^2} g_h(x, t) \leq \frac{1}{h^3} e^{-x^2/2Da_hh^2} e^{O(1/a_h^3 h^4)}.$$

Since $a_h = h^{-1-\mu}$, $\mu \in (0, 1)$, we see that the last exponential will approach 1 as $h \to 0$ if $\mu > 1/3$. Recall that μ must also satisfy the two inequalities given in (B.16). The choice of $\mu = 3/4$ given earlier satisfies all required inequalities. We have therefore shown that for all h sufficiently small,

$$G_h(\boldsymbol{x_j}, t) \leq \frac{C}{h^3} e^{-x^2/4Da_hh^2} \quad \forall t \in [0, a_hh^2).$$

This bound, coupled with the continuity in time of $G(\boldsymbol{x_j}, t)$ for $\boldsymbol{x_j} \neq 0$, then proves (B.9) and completes the proof of uniform convergence in time. ∎

COROLLARY B.2. *Let $\boldsymbol{x_j} = \boldsymbol{j}h$ be fixed as $h \to 0$, and let $\boldsymbol{x_j} \neq \boldsymbol{0}$. Then for all h sufficiently small and any $\epsilon > 0$ sufficiently small,*

$$\sup_{t\in[0,\infty)} |G_h(\boldsymbol{x_j}, t) - G(\boldsymbol{x_j}, t)| \leq Ch^{2-\epsilon}, \tag{B.17}$$

where C is independent of t and h.

Proof. We note that the choices $\mu = 1 - \epsilon/4$ and $\alpha = \epsilon/4$ satisfy all required inequalities in Theorem B.1. Moreover, all the necessary error terms will converge to zero exponentially as $h \to 0$ with the exception of the error bound on I_a given in (B.14). With the chosen μ and α this term satisfies

$$I_a \leq Ch^{2-\epsilon},$$

proving the corollary. ∎

Appendix C. Numerical methods for evaluating $p_h(x,t)$ and $p_h^{(i)}(x,t)$. All reported simulations were performed using MATLAB. The numerical calculations in both subsections 2.1 and 2.2.3 rely on evaluation of $G_h(\boldsymbol{x}, t)$, the Green's function for the discrete-space continuous-time diffusion equation, given by (2.8). To rapidly, and accurately, evaluate this function we rewrite it as

$$G_h(\boldsymbol{x}, t) = \prod_{k=1}^{3} g_h(x_k, t),$$

where

$$g_h(x_k, t) = 2\int_0^{1/2h} e^{-4Dt\sin(\pi h\xi_k)/h^2} \cos(2\pi x_k \xi_k)\, d\xi_k.$$

For the numerical calculations in subsection 2.2.3 we evaluated $g_h(x_k, t)$ using MATLAB's built-in adaptive Gauss–Lobato quadrature routine, `quadl`. This routine was found to be too slow for the repeated evaluations required in the calculations of subsection 2.1. There we instead numerically evaluated $g_h(x_k, t)$ using the trapezoidal rule, after applying the double exponential transformation for a finite interval described in [35]. For similar absolute error tolerances this method was substantially faster than `quadl`.

In subsection 2.1, $p_h(\boldsymbol{0}, t)$ was found using a Gregory method [13] to solve the Volterra equation of the second kind, (2.12). We found it necessary to use a sixth order method to resolve $p_h(\boldsymbol{0}, t)$ accurately with a computationally tractable number of time-points. For comparison, the fourth order Gregory method described in [13] would have required more time-points than available memory on our computer system to achieve the desired absolute error tolerance.

The sixth order Gregory method we used is based on discretizing time, $t_n = n\Delta t$, and calculating an approximate solution, $u_n(\boldsymbol{0}) \approx p_h(\boldsymbol{0}, t_n)$. The discrete equations satisfied by $u_n(\boldsymbol{0})$ are

$$u_n(\boldsymbol{0}) = G_h(\boldsymbol{x}_0, t_n) - k\Delta t \sum_{n'=0}^{n} G_h(\boldsymbol{0}, t_n - t_{n'}) u_{n'}(\boldsymbol{0})\, \omega_{n'}, \tag{C.1}$$

TABLE C.1
Gregory method weights, $\omega_{n'}$, for $n' = 0, \ldots, n$.

n'	$0, n$	$1, n-1$	$2, n-2$	$3, n-3$	$4, n-4$	$4 < n' < n-4$
$\omega_{n'}$	$\frac{95}{288}$	$\frac{317}{240}$	$\frac{23}{30}$	$\frac{793}{720}$	$\frac{157}{160}$	1

where the weights of the Gregory rule are given by Table C.1. To start this method we require values for $u_0(\mathbf{0}), u_1(\mathbf{0}), \ldots, u_8(\mathbf{0})$. $u_0(\mathbf{0})$ is given by the initial condition

$$u_0(\mathbf{0}) = G_h(\boldsymbol{x}_0, 0) = 0.$$

The other values were obtained by using a sixth order explicit Runge–Kutta method. (See [13] for details of using explicit Runge–Kutta methods to solve Volterra integral equations of the second kind, and [32] for the specific method we used.)

If one naively solves (C.1) by advancing from one time to the next, using $u_0(\mathbf{0})$, $\ldots$, $u_{n-1}(\mathbf{0})$ to calculate $u_n(\mathbf{0})$, the total work in solving for N time points will be $O(N^2)$. The discrete convolution structure of (C.1) can be exploited by the FFT-based method of [22] to reduce the total work to $O(N \log^2(N))$. In practice we required this optimization to solve (C.1) in a reasonable amount of time. An important technical point that we found was that both MATLAB's built-in discrete convolution routine, `conv`, and the MATLAB Signaling Toolbox FFT-based method, `fftfilt`, performed poorly for sufficiently large vectors. Our final code used the `convfft` routine [41], which performed significantly faster for large vectors.

We found this solution method computationally effective for h as small as 2^{-11}. Below this mesh size we encountered stability problems with the Gregory discretization. Moreover, to obtain the same absolute error tolerances used for coarser mesh sizes, the simulations required more time-points than could be stored in the four gigabytes of system memory on our workstation. We also tried several [36, 45] existing spectral methods for numerically solving Volterra integral equations of the second kind, but found that in practice they were unable to obtain accuracies comparable to those of the Gregory method described above in solving (2.12).

Once $u_n(\mathbf{0})$ was calculated, we solved for $u_n(\boldsymbol{x}) \approx p_h(\boldsymbol{x}, t_n)$ by discretizing (2.11) to give

$$u_n(\boldsymbol{x}) = G_h(\boldsymbol{x} - \boldsymbol{x}_0, t) - k\Delta t \sum_{n'=0}^{n} G_h(\boldsymbol{x}, t_n - t_{n'}) u_{n'}(\mathbf{0})\, \omega_{n'},$$

where $\omega_{n'}$ is again defined by Table C.1.

Finally, for the figures in subsection 2.2.3 each value of $p_h^{(1)}(\boldsymbol{x}, t)$ was calculated using the composite Simpson's rule. $p_h^{(2)}(\boldsymbol{x}, t)$ was calculated by reusing the composite Simpson's rule on the calculated values of $p_h^{(1)}(\boldsymbol{x}, t)$.

Acknowledgments. The author would like to thank several individuals for helpful discussions. Charles Peskin helped stimulate this work through discussions on the nature of the continuum limit of the RDME. In particular, he showed by Laplace transform methods that the mean binding time for a bimolecular reaction in the RDME with periodic geometry becomes infinite as the mesh spacing approaches zero, suggesting the approach of section 2.1. David Isaacson aided the author in developing an alternative derivation of the asymptotic expansion of the solution to the SCDLR model through the use of pseudopotentials; see [27]. Both David Isaacson and Charles

Peskin provided critical comments on this manuscript. Firas Rassoul-Agha suggested both the time splitting used in the uniform convergence proof of Theorem B.1 and the bounding by an exponential trick used in the short-time part of the proof. He also provided a separate proof of the uniform convergence for large times through a different argument, based on extending the local central limit theorem for discrete-time random walks to continuous-time random walks.

Finally, we would like to thank Bob Guy, James P. Keener, and Eric Vanden-Eijnden for helpful discussions, and the referees for their helpful comments. In particular, Appendix A was added due to suggestions of one referee.

REFERENCES

[1] M. Abramowitz and I. A. Stegun, *Handbook of Mathematical Functions with Formulas, Graphs, and Mathematical Tables*, Dover Publications, New York, 1965.
[2] J. L. Adelman and S. Andrews, *Intracellular pattern formation: A spatial stochastic model of bacterial division site selection proteins MinCDE*, in Proceedings of the Santa Fe Institute Summer School, 2004; see http://www.smoldyn.org/andrews/publications.html.
[3] S. Albeverio, Z. Brzeźniak, and L. Dąbrowski, *Fundamental solution of the heat and Schrödinger equations with point interaction*, J. Funct. Anal., 130 (1995), pp. 220–254.
[4] S. Albeverio, F. Gesztesy, R. Høegh-Krohn, and H. Holden, *Solvable Models in Quantum Mechanics*, 2nd ed., AMS Chelsea, New York, 1988.
[5] S. Albeverio and P. Kurasov, *Singular Perturbations of Differential Operators*, London Math. Soc. Lecture Note Ser. 271, Cambridge University Press, New York, 2000.
[6] S. S. Andrews and D. Bray, *Stochastic simulation of chemical reactions with spatial resolution and single molecule detail*, Phys. Biol., 1 (2004), pp. 137–151.
[7] A. Arkin and H. H. McAdams, *Stochastic mechanisms in gene expression*, Proc. Natl. Acad. Sci. USA, 94 (1997), pp. 814–819.
[8] A. Arkin, J. Ross, and H. H. McAdams, *Stochastic kinetic analysis of developmental pathway bifurcation in phage λ-infected* Escherichia coli *cells*, Genetics, 149 (1998), pp. 1633–1648.
[9] F. Baras and M. M. Mansour, *Reaction-diffusion master equation: A comparison with microscopic simulations*, Phys. Rev. E, 54 (1996), pp. 6139–6147.
[10] F. Berezin and L. Faddeev, *A remark on Schrödinger equation with a singular potential*, Soviet Math. Dokl., 2 (1961), pp. 372–375.
[11] U. S. Bhalla, *Signaling in small subcellular volumes.* I. *Stochastic and diffusion effects on individual pathways*, Biophys. J., 87 (2004), pp. 733–744.
[12] W. J. Blake, M. Kaern, C. R. Cantor, and J. J. Collins, *Noise in eukaryotic gene expression*, Nature, 422 (2003), pp. 633–637.
[13] L. M. Delves and J. L. Mohamed, *Computational Methods for Integral Equations*, Cambridge University Press, Cambridge, UK, 1985.
[14] M. Doi, *Second quantization representation for classical many-particle system*, J. Phys. A: Math. Gen., 9 (1976), pp. 1465–1477.
[15] J. Elf and M. Ehrenberg, *Spontaneous separation of bi-stable biochemical systems into spatial domains of opposite phases*, IEE Sys. Biol., 1 (2004), pp. 230–236.
[16] R. Erban, S. J. Chapman, and P. K. Maini, *A Practical Guide to Stochastic Simulations of Reaction-Diffusion Processes*, lecture notes, available online at http://www2.maths.ox.ac.uk/~erban/papers/download.html.
[17] D. Fange and J. Elf, *Noise induced min phenotypes in E. coli*, PLoS Comput. Biol., 2 (2006), pp. 0637–0638.
[18] W. Feller, *An Introduction to Probability Theory and Its Applications*, Vol. II, John Wiley & Sons, New York, 1971.
[19] E. Fermi, *Motion of neutrons in hydrogenous substances*, Ricerca Sci., 7 (1936), pp. 13–52.
[20] C. W. Gardiner, K. J. McNeil, D. F. Walls, and I. S. Matheson, *Correlations in stochastic theories of chemical reactions*, J. Statist. Phys., 14 (1976), pp. 307–331.
[21] D. T. Gillespie, *Exact stochastic simulation of coupled chemical-reactions*, J. Phys. Chem., 81 (1977), pp. 2340–2361.
[22] E. Hairer, Ch. Lubich, and M. Schlichte, *Fast numerical solution of nonlinear Volterra convolution equations*, SIAM J. Sci. Stat. Comput., 6 (1985), pp. 532–541.
[23] M. Hazewinkel, ed., *Encyclopaedia of Mathematics*, Springer-Verlag, New York, Berlin, 2002.
[24] K. Huang and C. N. Yang, *Quantum-mechanical many-body problem with hard-sphere interaction*, Phys. Rev., 105 (1957), pp. 767–775.

[25] S. A. Isaacson, *A Stochastic Reaction–Diffusion Method for Studying the Control of Gene Expression in Eukaryotic Cells*, Ph.D. thesis, Department of Mathematics, New York University, New York, 2005.

[26] S. A. Isaacson, *Relationship between the reaction-diffusion master equation and particle tracking models*, J. Phys. A, 41 (2008), paper 065003.

[27] S. A. Isaacson and D. Isaacson, *The Reaction-Diffusion Master Equation, Diffusion Limited Reactions, and Singular Potentials*, manuscript.

[28] S. A. Isaacson and C. S. Peskin, *Incorporating diffusion in complex geometries into stochastic chemical kinetics simulations*, SIAM J. Sci. Comput., 28 (2006), pp. 47–74.

[29] J. Keizer, *Nonequilibrium statistical thermodynamics and the effect of diffusion on chemical reaction rates*, J. Phys. Chem., 86 (1982), pp. 5052–5067.

[30] F. Kühner, L. T. Costa, P. M. Bisch, S. Thalhammer, W. M. Heckl, and H. E. Gaub, *LexA-DNA bond strength by single molecule force spectroscopy*, Biophys. J., 87 (2004), pp. 2683–2690.

[31] G. Lahav, N. Rosenfeld, A. Sigal, N. Geva-Zatorsky, A. J. Levine, M. B. Elowitz, and U. Alon, *Dynamics of the p53-Mdm2 feedback loop in individual cells*, Nature Genetics, 36 (2004), pp. 147–150.

[32] H. A. Luther, *An explicit sixth-order Runge-Kutta formula*, Math. Comp., 22 (1968), pp. 434–436.

[33] H. Maamar, A. Raj, and D. Dubnau, *Noise in gene expression determines cell fate in* Bacillus subtilis, Science, 317 (2007), pp. 526–529.

[34] D. A. McQuarrie, *Stochastic approach to chemical kinetics*, J. Appl. Probab., 4 (1967), pp. 413–478.

[35] M. Mori and M. Sugihara, *The double-exponential transformation in numerical analysis*, J. Comput. Appl. Math., 127 (2001), pp. 287–296.

[36] M. Muhammad, A. Nurmuhammad, M. Mori, and M. Sugihara, *Numerical solution of integral equations by means of the sinc collocation method based on the double exponential transformation*, J. Comput. Appl. Math., 177 (2005), pp. 269–286.

[37] E. M. Ozbudak, M. Thattai, I. Kurtser, A. D. Grossman, and A. van Oudenaarden, *Regulation of noise in the expression of a single gene*, Nature Genetics, 31 (2002), pp. 69–73.

[38] N. Pavin, H. v. Paljetak, and V. Krstić, *Min-protein oscillations in* Escherichia coli *with spontaneous formation of two-stranded filaments in a three-dimensional stochastic reaction-diffusion model*, Phys. Rev. E, 73 (2006), paper 021904.

[39] L. Peliti, *Path integral approach to birth-death processes on a lattice*, J. Physique, 46 (1985), pp. 1469–1483.

[40] J. M. Raser and E. K. O'Shea, *Control of stochasticity in eukaryotic gene expression*, Science, 304 (2004), pp. 1811–1814.

[41] L. Rosa, `fftconv.m`, *MATLAB program*, available online at http://www.mathworks.com/matlabcentral/fileexchange.

[42] A. E. Smith, B. M. Slepchenko, J. C. Schaff, L. M. Loew, and I. G. Macara, *Systems analysis of Ran transport*, Science, 295 (2002), pp. 488–491.

[43] M. V. Smoluchowski, *Mathematical theory of the kinetics of the coagulation of colloidal solutions*, Z. Phys. Chem., 92 (1917), pp. 129–168.

[44] G. M. Süel, J. G. Garcia-Ojalvo, L. M. Liberman, and M. B. Elowitz, *An excitable gene regulatory circuit induces transient cellular differentiation*, Nature, 440 (2005), pp. 545–550.

[45] T. Tang, X. Xu, and J. Cheng, *On spectral methods for Volterra type integral equations and the convergence analysis*, J. Comput. Math., 26 (2008), pp. 825–837.

[46] U. C. Täuber, M. Howard, and B. P. Vollmayr-Lee, *Applications of field-theoretic renormalization group methods to reaction-diffusion problems*, J. Phys. A, 38 (2005), pp. R79–R131.

[47] J. S. van Zon, M. J. Morelli, S. Tănase-Nicola, and P. R. ten Wolde, *Diffusion of transcription factors can drastically enhance the noise in gene expression*, Biophys. J., 91 (2006), pp. 4350–4367.

[48] J. S. van Zon and P. R. ten Wolde, *Simulating biochemical networks at the particle level and in time and space: Green's function reaction dynamics*, Phys. Rev. Lett., 94 (2005), paper 128103.